

Manuscript Number: FSIM-D-12-00522R2

Title: Transgene and immune gene expression following intramuscular injection of Atlantic salmon (*Salmo salar* L.) with DNA-releasing PLGA nano- and microparticles

Article Type: Full Length Article

Keywords: PLGA; Nanoparticles; Microparticles; Transgene expression; Immune responses

Corresponding Author: Dr. Roy Ambli Dalmo, PhD

Corresponding Author's Institution: BFE Faculty

First Author: Linn Benjaminsen Hølvold

Order of Authors: Linn Benjaminsen Hølvold; Børge N. Fredriksen; Jarl Bøggwald; Roy A Dalmo, PhD

**Abstract:** The use of poly-(D,L-lactic-co-glycolic) acid (PLGA) particles as carriers for DNA delivery has received considerable attention in mammalian studies. DNA vaccination of fish has been shown to elicit durable transgene expression, but no reports exist on intramuscular administration of PLGA-encapsulated plasmid DNA (pDNA). We injected Atlantic salmon (*Salmo salar* L.) intramuscularly with a plasmid vector containing a luciferase (*Photinus pyralis*) reporter gene as a) naked pDNA, b) encapsulated into PLGA nano- (~320nm) (NP) or microparticles (~4µm) (MP), c) in an oil-based formulation, or with empty particles of both sizes. The ability of the different pDNA-treatments to induce transgene expression was analyzed through a 70-day experimental period. Anatomical distribution patterns and depot effects were determined by tracking isotope labeled pDNA. Muscle, head kidney and spleen from all treatment groups were analyzed for proinflammatory cytokines (TNF $\alpha$ , IL-1 $\beta$ ), antiviral genes (IFN- $\alpha$ , Mx) and cytotoxic T-cell markers (CD8, Eomes) at mRNA transcription levels at days 1, 2, 4 and 7. Histopathological examinations were performed on injection-site samples from days 2, 7 and 30. Injection of either naked pDNA or the oil-formulation was superior to particle treatments for inducing transgene expression at early time-points. Empty particles of both sizes were able to induce proinflammatory immune responses as well as degenerative and inflammatory pathology at the injection site. Microparticles demonstrated injection-site depots and an inflammatory pathology comparable to the oil-based formulation. In comparison, the distribution of NP-encapsulated pDNA resembled that of naked pDNA, although encapsulation into NPs significantly elevated the expression of antiviral genes in all tissues. Together the results indicate that while naked pDNA is most efficient for inducing transgene expression, the encapsulation of pDNA into NPs up-regulates antiviral responses that could be of benefit to DNA vaccination.

## Highlights

- Plasmid DNA was encapsulated into PLGA nano- and microparticles
- Naked and encapsulated pDNA was injected into muscle of Atlantic salmon
- Naked pDNA delivery is superior for inducing transgene expression
- Nano- and microparticles induce significant expression of inflammatory genes
- Nanoparticles carrying pDNA significantly up-regulate antiviral genes

**Table 1 – An overview of the preparation protocol and main particle characteristics for pDNA-loaded PLGA nanoparticles (NP-(<sup>125</sup>I-f-pDNA)) and microparticles (MP-(<sup>125</sup>I-f-pDNA)). (S): preparation by sonication. (H): preparation by homogenization. Preparation of empty particles followed the same protocol, but pDNA was excluded from the W<sub>1</sub> phase.**

	NP-( <sup>125</sup> I-f-pDNA)	MP-( <sup>125</sup> I-f-pDNA)
First water phase (W <sub>1</sub> )	pDNA (3.5 mg) in 600 µl dH <sub>2</sub> O with 0.1% PVA	
Oil phase (O)	300 mg PLGA in 6 ml chloroform (5% w/v)	
First emulsion (W <sub>1</sub> /O)	S: 30 sec, 35% (262.5 W)	S: 35 sec, 30% (225 W)
Second water phase (W <sub>2</sub> )	15 ml dH <sub>2</sub> O with 2% PVA	
Second emulsion (O/W <sub>2</sub> )	S: 1 min, 30%	H: 45 sec, 9500 rpm min <sup>-1</sup>
Washing	5000 x g, 15000 x g and 25000 x g	500 x g
Particle yield (%)	78	89
Encapsulation efficiency (%)	27	24
Loading (µg pDNA/mg PLGA)	3.24	2.85
Mean size	320 nm	3-4 µm
PLGA injected (mg)	3.5	4

**Table 2 - Experimental groups and group nomenclature.**

Treatment groups	Nomenclature
( <sup>125</sup> I-f-pDNA) encapsulated in nanoparticles	NP-( <sup>125</sup> I-f-pDNA)
( <sup>125</sup> I-f-pDNA) encapsulated in microparticles	MP-( <sup>125</sup> I-f-pDNA)
Empty nanoparticles	NP
Empty microparticles	MP
Plasmid DNA in PBS	pDNA
( <sup>125</sup> I-f-pDNA) in PBS	<sup>125</sup> I-f-pDNA
PBS	PBS
( <sup>125</sup> I-f-pDNA) in Freund's incomplete adjuvant	FIA-( <sup>125</sup> I-f-pDNA)

**Table 3 - Primers for quantitative polymerase chain reaction (QPCR). (\*): primers obtained from Natasha Hynes (TNF- $\alpha$ ) and Jaya Kumari (Eomes).**

Primer		Oligonucleotides, 5' to 3'	GenBank accession number	Concentration (nM)	Amplification efficiency (%)	Amplicon size (bp)
EF1A <sup>1</sup>	Fw	CACCACCGCCATCTGATCTACAA	AF321836	150	93	78
	Rv	TCAGCAGCCTCCTTCTCGAACTTC		150		
Luc <sup>2</sup>	Fw	TGGGCTCACTGAGACTACATCA	M15077.1	900	100	64
	Rv	CGCGCCCGGTTTATCATC		900		
TNF $\alpha$ <sup>*</sup>	Fw	TGTCCATCAAGCCACTACACTC	BT049358	250	84	129
	Rv	GCACTCACACACCTGTCATT		250		
IFN $\alpha$ <sup>1</sup>	Fw	TGGGAGGAGATATCACAAAGC	NM_001123570	250	89	163
	Rv	TCCCAGGTGACAGATTTTCAT		250		
IL-1 $\beta$ <sup>1</sup>	Fw	GCTGGAGAGTGCTGTGGAAGA	AY617117	200	104	73
	Rv	TGCTTCCCTCCTGCTCGTAG		200		
CD8 $\alpha$ <sup>3</sup>	Fw	CGTCTACAGCTGTGCATCAATCAA	AY693391	200	83	266
	Rv	GGCTGTGGTCATTGGTGTAGTC		200		
Eomes <sup>*</sup>	Fw	ACCTCTCGTCGTCAGATAGTG	NM_001204100	200	82	204
	Rv	GGACCGGTGAGTCTTTTCTTC		200		
Mx <sup>4</sup>	Fw	TGCAACCACAGAGGCTTTGAA	NM_001139918	200	92	79
	Rv	GGCTTGGTCAGGATGCCTAAT		200		

**Table 4 - Histopathological observations in tissue-sections of muscle from the injection site. Muscle degeneration and inflammation are classified as either moderate (+) or strong (++), depending on the extent of the pathology.**

Sampling	Group	Total number of fish	Hemorrhage	Muscle degeneration		Inflammation	
				+	++	+	++
D2	NP-( <sup>125</sup> I-f-pDNA)	3	2	2	0	0	0
	MP-( <sup>125</sup> I-f-pDNA)	3	2	3	0	2	0
	NP	2	1	1	1	0	0
	MP	3	2	0	2	0	0
	pDNA	3	1	1	2	0	0
	<sup>125</sup> I-f-pDNA	3	2	0	0	0	0
	PBS	2	1	2	0	0	0
	FIA-( <sup>125</sup> I-f-pDNA)	1	-	1	-	-	-
D7	NP-( <sup>125</sup> I-f-pDNA)	3	2	2	0	2	0
	MP-( <sup>125</sup> I-f-pDNA)	3	0	3	0	2	0
	NP	2	0	1	1	2	0
	MP	2	1	2	0	2	0
	pDNA	3	1	2	0	1	0
	<sup>125</sup> I-f-pDNA	3	2	1	0	0	0
	PBS	2	0	0	0	0	0
	FIA-( <sup>125</sup> I-f-pDNA)	1	-	-	-	-	-
D30	NP-( <sup>125</sup> I-f-pDNA)	2	0	0	0	2	0
	MP-( <sup>125</sup> I-f-pDNA)	2	0	1	1	0	2
	pDNA	2	0	0	0	2	0
	<sup>125</sup> I-f-pDNA	2	0	0	0	0	0
	PBS	1	0	0	0	0	0
	FIA-( <sup>125</sup> I-f-pDNA)	1	-	-	-	-	1

**Dear Editors,**

Please find enclosed a revised manuscript of “**Transgene and immune gene expression following intramuscular injection of Atlantic salmon (*Salmo salar* L.) with DNA-releasing PLGA nano- and microparticles**” by Linn Benjaminsen Hølvold, Børge N. Fredriksen, Jarl Bøggwald and Roy A. Dalmo, which we are re-submitting for consideration for publication in *Fish and Shellfish Immunology*.

Our study is the first on intramuscular injection of DNA-releasing PLGA particles in Atlantic salmon. We aimed to evaluate the effect that encapsulation of pDNA into PLGA nano- and microparticles would have not only on transgene expression, but also on immune responses that might modulate the efficacy of the expressed transgene, as well as tissue distribution and injection site depots. DNA vaccination has been shown to induce protective immune responses in Atlantic salmon, and research on vaccine strategies to further improve the efficacy of DNA vaccines should therefore be of interest to the readers of *Fish and Shellfish Immunology*.

The manuscript has been revised in accordance with the received comments from reviewers.

All authors contributed to the work described in the paper, and take responsibility for it. Further, none of the described work has been published elsewhere.

We would be grateful if you would consider this revised manuscript for publication in your journal.

Sincerely,

Linn Benjaminsen Hølvold



24 **Abstract**

25 The use of poly-(D,L-lactic-*co*-glycolic) acid (PLGA) particles as carriers for DNA  
26 delivery has received considerable attention in mammalian studies. DNA vaccination of  
27 fish has been shown to elicit durable transgene expression, but no reports exist on  
28 intramuscular administration of PLGA-encapsulated plasmid DNA (pDNA). We injected  
29 Atlantic salmon (*Salmo salar* L.) intramuscularly with a plasmid vector containing a  
30 luciferase (*Photinus pyralis*) reporter gene as a) naked pDNA, b) encapsulated into  
31 PLGA nano- (~320nm) (NP) or microparticles (~4µm) (MP), c) in an oil-based  
32 formulation, or with empty particles of both sizes. The ability of the different pDNA-  
33 treatments to induce transgene expression was analyzed through a 70-day experimental  
34 period. Anatomical distribution patterns and depot effects were determined by tracking  
35 isotope labeled pDNA. Muscle, head kidney and spleen from all treatment groups were  
36 analyzed for proinflammatory cytokines (TNF $\alpha$ , IL-1 $\beta$ ), antiviral genes (IFN- $\alpha$ , Mx) and  
37 cytotoxic T-cell markers (CD8, Eomes) at mRNA transcription levels at days 1, 2, 4 and  
38 7. Histopathological examinations were performed on injection-site samples from days 2,  
39 7 and 30. Injection of either naked pDNA or the oil-formulation was superior to particle  
40 treatments for inducing transgene expression at early time-points. Empty particles of both  
41 sizes were able to induce proinflammatory immune responses as well as degenerative and  
42 inflammatory pathology at the injection site. Microparticles demonstrated injection-site  
43 depots and an inflammatory pathology comparable to the oil-based formulation. In  
44 comparison, the distribution of NP-encapsulated pDNA resembled that of naked pDNA,  
45 although encapsulation into NPs significantly elevated the expression of antiviral genes  
46 in all tissues. Together the results indicate that while naked pDNA is most efficient for



47 inducing transgene expression, the encapsulation of pDNA into NPs up-regulates  
48 antiviral responses that could be of benefit to DNA vaccination.

49

50

51

52

53

54

55

56

57

58

59

60

61

62

63

64

65

66

67

68

69

70 **Introduction**

71 PLGA (poly-(D,L-lactic-*co*-glycolic)-acid) nano- and microparticles as adjuvants and  
72 carriers for vaccine antigens have been extensively investigated, mainly in mammalian  
73 models [1-5]. The biodegradable copolymer produces non-toxic degradation products [3],  
74 offers increased predictability of antigen release-rates, potential for intracellular antigen  
75 delivery and the ability to encapsulate and co-encapsulate a wide variety of antigens,  
76 including DNA vaccines [1, 6, 7].

77 **Luciferase has commonly been applied for the evaluation of DNA vaccines at**  
78 **both transcription and protein level, and appears to express higher in fish than in**  
79 **mammals for a given dose of DNA** [8-12]. The encapsulation of plasmid DNA into  
80 PLGA particles could protect against the rapid on-site degradation reported in both mice  
81 and salmon after intramuscular injection, and has been shown to increase the escape of  
82 antigen from endosomes to the cytosol [6, 8, 10, 11, 13].

83 Depending on size, the particles may create injection-site depots (>5 $\mu$ m), get  
84 phagocytized by antigen presenting cells (APCs) (<5 $\mu$ m), be internalized by non-  
85 phagocytic cells such as myocytes (<500nm) or escape into the bloodstream and  
86 subsequently be cleared by phagocytes in the head kidney, spleen and/or liver [4, 14].  
87 Muscle cells have been shown to slowly accumulate pDNA over time, and could benefit  
88 from extracellular pDNA-releasing microparticles as well as intracellular nanoparticle  
89 depots [15].

90 A central attribute of DNA vaccines is the ability to induce cellular as well as  
91 humoral immune responses, including cytotoxic T-lymphocyte (CTL) responses and  
92 antibody production [16-18]. Unlike vertebrate DNA, bacterial DNA contains stretches of

93 unmethylated CpG sequences that are recognized as danger signals by toll-like receptor 9  
94 (TLR9). Upon stimulation this endosomal pattern recognition receptor (PRR) may induce  
95 a variety of cytokines. Interleukin-1 $\beta$  (IL-1 $\beta$ ) and tumor necrosis factor- $\alpha$  (TNF- $\alpha$ ) are  
96 hallmark cytokines in driving the inflammatory response in mammals and amongst other  
97 properties hold key roles in the migration of effector cells to sites of infection [19]. Both  
98 cytokines have been found in a number of teleost species and appear to exert functions  
99 similar to what is known from mammals [20-22].

100 Interferon- $\alpha$  (IFN- $\alpha$ ) is one of the type I IFNs, key mediators of antiviral  
101 responses through the regulation of IFN-stimulated genes and central in linking innate  
102 and adaptive immunity [16, 23-25]. The IFN-induced protein Mx has demonstrated  
103 antiviral functions in Atlantic salmon (*Salmo salar* L.) and can be used to follow IFN  
104 activity, as it has a much longer lifetime and accumulates to higher concentrations [26-  
105 28]. Type I IFNs also play an important role in the clonal expansion and generation of  
106 specific as well as non-specific memory CD8<sup>+</sup> T-cells [29]. Sequences for CD8 $\alpha$  and  
107 CD8 $\beta$  are known from a variety of teleost species and the cytotoxic activity of CD8<sup>+</sup> T-  
108 cells has been demonstrated in rainbow trout (*Oncorhynchus mykiss*) [30, 31]. The  
109 transcription factor Eomesodermin (Eomes) is critical to the development of CD8<sup>+</sup> T-cell  
110 effector functions and memory cells in mammals [32, 33]. A recent study indicated  
111 similar functions as well as induction by IFN- $\alpha$  in Atlantic salmon [34].

112 Intramuscular injection of naked pDNA generally induces few and transient  
113 histopathological changes in fish as well as in mammals [9]. In contrast, the use of PLG  
114 microspheres as DNA carriers has been shown to result in a foreign body response in  
115 mice, where the infiltrating cells were also the ones that were primarily transfected [35].

116 Enhanced inflammatory reactions coupled with prolonged availability of pDNA might  
117 therefore be beneficial to transgene expression and T-cell responses.

118 This report is the first on intramuscular injection of Atlantic salmon with PLGA  
119 nano- and microparticles carrying pDNA, and the effect of these particles on 1) tissue  
120 distribution and retention of pDNA 2) expression of a firefly (*Photinus pyralis*) luciferase  
121 reporter gene 3) innate inflammatory (TNF- $\alpha$ , IL-1 $\beta$ ) and antiviral (IFN- $\alpha$ , Mx) immune  
122 responses, 4) expression of cytotoxic T-cell markers (CD8, Eomes) and 5) injection site  
123 histopathology. We hypothesize that PLGA-encapsulated pDNA will induce transgene  
124 expression and proinflammatory as well as antiviral responses more efficiently than non-  
125 encapsulated pDNA.

126

127

## 128 **2. Experimental**

### 129 *2.1 Materials/Chemicals*

130 Poly(D,L-lactic-co-glycolic) acid (PLGA; 50:50 ratio,  $M_w$  of 7-17 kDa), poly vinyl  
131 alcohol (PVA, 87-89 % hydrolyzed), D-(+)-trehalose dehydrate, 1,3,4,6-tetrachloro-3 $\alpha$ ,  
132 6 $\alpha$ -diphenylglycouril (Iodogen; Pierce, Rockford, IL, USA), Freund's incomplete  
133 adjuvant (FIA) and quantitative polymerase chain-reaction (QPCR) primers were  
134 purchased from Sigma Aldrich. Carrier free Na[<sup>125</sup>I] was from Perkin-Elmer Norge  
135 (Oslo, Norway). Acetone, dichloromethane (DCM) and chloroform were purchased from  
136 Merck Biochemicals. Sodium metabisulphite (Na<sub>2</sub>S<sub>2</sub>O<sub>5</sub> > 98 % purity) and potassium  
137 iodide (KI > 99.5 % purity) were purchased from Fluka Biochemica. Luciferase  
138 lyophilizate was purchased from Roche Diagnostics GmbH (Mannheim, Germany).

139 2.2 *Plasmid DNA*

140 Plasmid R70pRomiLuc (gift from Uwe Fischer, Friedrich-Loeffler-Institut, Germany)  
141 contains a firefly luciferase gene under the control of a murine cytomegalovirus  
142 immediate early promoter (CMV-IEP). The plasmid was isolated from a culture of  
143 *Escherichia coli* (strain DH5 $\alpha$ ) by use of Qiagen Plasmid Giga Kit (Qiagen GmbH,  
144 Hilden, Germany) according to manufacturer instructions. Purified plasmid was eluted in  
145 Tris-EDTA (TE) buffer (pH=8.0). DNA concentration and quality was determined with a  
146 NanoDrop® ND-1000 spectrophotometer (NanoDrop Technologies, Wilmington, DE,  
147 USA) and 1% agarose gel-electrophoresis. High quality samples ( $A_{260}/A_{280}$  ratio > 1.9  
148 and distinct DNA bands on gel) were stored at -20 °C until use.

149

150 2.3 *Preparation of [<sup>125</sup>I]-fluorescein-pDNA*

151 Purified pDNA was modified using the nucleic acid labeling kit *LabelIT* Fluorescein  
152 (MIR 3200, Mirus Corp., Madison, WI, USA) according to manufacturer instructions.  
153 Radiolabeling of f-pDNA with carrier-free Na[<sup>125</sup>I] was performed in a direct reaction  
154 with 1,3,4,6-tetrachloro-3 $\alpha$ ,6 $\alpha$ -diphenylglycoluril as the oxidizing agent. The protocol  
155 was in accordance with the Iodogen method of radiolabeling [36], with minor  
156 modifications concerning incubation time (1h). Free iodine was removed by filtration on  
157 a PD-10 column equilibrated with pDNA in PBS. Radiation was determined by gamma  
158 counting (COBRA™ II Auto-Gamma®, ©Packard Instrument Co., Meridan, IL, USA),  
159 with specific activity measured to ~ 4.75 million cpm  $\mu\text{g}^{-1}$  <sup>125</sup>I-f-pDNA.

160

161

162 *2.4 Preparation of naked and pDNA-loaded nano- and microparticles*

163 Particles were prepared by a modified version of the double emulsion ( $W_1/O/W_2$ ) solvent  
164 evaporation method [2, 5, 37], outlined in table 1. A fraction of  $^{125}\text{I}$ -f-pDNA was  
165 included in the first water phase ( $W_1$ ) for determination of encapsulation efficiency and  
166 tracing of tissue distribution in *in vivo* experiments. Emulsions were prepared on ice-  
167 baths by sonication (S) (Sonics VibraCell VC750, 3 mm tapered micro tip, Sonics &  
168 Materials Inc., Newtown, CT, USA) or homogenization (H) (Ultra-turrax® T-25 Basic,  
169 IKA®-WERKE, Staufen, Germany). Plasmid was excluded from the  $W_1$  phase for  
170 preparation of naked particles. Fifteen ml  $\text{dH}_2\text{O}$  was added to the  $W_1/O/W_2$ -emulsions  
171 before overnight stirring to facilitate solvent evaporation. After centrifugation (Avanti®  
172 J-26 XP, BeckmanCoulter®, USA), pellets were resuspended in  $\text{dH}_2\text{O}$  and the fractions  
173 were pooled. Trehalose ( $5 \text{ mg ml}^{-1}$  in  $\text{dH}_2\text{O}$ ) was used as a lyoprotectant and added to  
174 suspension aliquots in a ratio of 1:3. Aliquots were kept at  $-80^\circ\text{C}$  for a minimum of 2 h  
175 before lyophilization for 72 h at 0.001 hPa,  $-110^\circ\text{C}$  (ScanVac CoolSafe™, LaboGene,  
176 Denmark). Lyophilizates were stored in airtight containers at  $4^\circ\text{C}$ .

177

178 *2.5 Particle characterization*

179 Encapsulation of pDNA was determined by the gamma emission in a known amount of  
180 particles (COBRA™ II Auto-Gamma®) and measured radioactivity related to the  
181 specific radioactivity in the fraction of  $^{125}\text{I}$ -f-pDNA stock solution added to the  $W_1$ -phase.  
182 Encapsulation efficiency was determined as entrapped amount of pDNA relative to the  
183 amount initially present in the  $W_1$ -phase. Loading ( $\mu\text{g pDNA mg}^{-1}$  PLGA) was calculated  
184 by relating encapsulated pDNA to the total weight of retrieved particles. Sizing of

185 nanoparticles was performed by photon correlation spectroscopy (PCS) (NiComp 380  
186 Submicron Particle Sizer, Santa Barbara, USA). Microparticle size was determined by  
187 use of a Model 780 AccuSizer (NiComp).

188

### 189 *2.6 In vitro particle stability and pDNA release*

190 Five containers of 10 mg lyophilizate dissolved in 1 ml PBS (pH 7.4) with 0.02% sodium  
191 azide (NaN<sub>3</sub>) were prepared for both nano- and microparticles. The suspensions were  
192 incubated at 8°C on a Stuart® SB3 rotator. Sampling was performed immediately after  
193 particles had been dissolved, and then at 3 h, day 1, 2, 4, 7, 14, 21, 30, 40, 50, 60 and 70.  
194 At each sampling 100 µl were removed and centrifuged at 15,000 x g for 1 minute. Fifty  
195 µl of the supernatant were removed for isotope measurement, and the remaining fraction  
196 transferred back to the original container after addition of 50 µl new PBS and full re-  
197 suspension of the particle pellets.

198

### 199 *2.7 Fish*

200 Unvaccinated pre-smolt Atlantic salmon with a mean weight of 30 g were provided by  
201 and kept at Tromsø Aquaculture Research Station. The fish were kept in 200 L plastic  
202 tanks supplied with running fresh water (8-10°C) and fed a commercial feed from  
203 Skretting AS (Stavanger, Norway). Adaptation to test conditions was performed for one  
204 week prior to immunization. All experiments were in compliance with The Norwegian  
205 Welfare of Animals Act.

206

207

208 *2.8 Experimental groups and vaccination*

209 A total of 336 fish were distributed among seven tanks. Each tank contained 6 fish from  
210 each of the eight experimental groups (Table 2). Prior to tattooing and immunization the  
211 fish were sedated with benzocaine using 40 mg L<sup>-1</sup> (Benzoak Vet., ACD  
212 Pharmaceuticals, Leknes, Norway). The PanJet needle free injection system with  
213 saturated Alcian blue was used for tattooing. All formulations were administered in 50 µl  
214 volumes by injection in the left epaxial muscle. Each injection dose contained 11 µg  
215 pDNA, and the amount of NPs and MPs was adjusted to make up for differences in  
216 pDNA loading. Injection dose samples were collected from each formulation in order to  
217 determine cpm.

218

219 *2.9 Sampling*

220 The fish were starved for 24 h prior to sampling and killed by a double dose (80 mg L<sup>-1</sup>)  
221 of benzocaine. At day 1, 2, 4, 7, 14, 30 and 70 post injection one tank was sampled. All  
222 fish were weighed. Blood from fish given radioactive formulations was sampled using  
223 vacutainers (Becton Dickinson) and stored on ice. Two muscle samples from the  
224 injection site were transferred to 10% neutral buffered formalin for storage until  
225 histological processing. Muscle samples, spleens and head kidneys were transferred to  
226 separate tubes containing 1 ml RNAlater® (Ambion, Austin, TX, USA) and kept at room  
227 temperature overnight before storage at -20°C. To determine tissue distribution in fish  
228 given radioactive formulations it was necessary to sample the full carcass. Trunk kidney,  
229 organ package (liver, heart, gastrointestinal tract (GIT) and interstitial adipose tissue),  
230 head (incl. gills) and remaining muscle (with skin) were collected in separate tubes. One



231 fish injected only with PBS was similarly sampled at each time point in order to exclude  
232 the possibility of radioactive contamination by cohabitation.

233

#### 234 *2.10 Anatomic distribution and plasmid DNA retention*

235 Determination of *in vivo* retention and biodistribution was achieved by tracking trace  
236 amounts of  $^{125}\text{I}$ -f-pDNA. From blood samples, 50  $\mu\text{l}$  were removed for analysis.  
237 Radioactivity in blood and trunk kidney samples was determined with a COBRA™ II  
238 gamma counter. Remaining samples, including spleen and injection site tissue, were  
239 analyzed using a Packard Auto-Gamma Scintillation Spectrometer (©Packard Instrument  
240 Co., model 5120). Background radiation was measured to be 50 and 100 cpm  
241 respectively for the two machines. These were set as baselines, and were subtracted from  
242 measured values before data were adjusted according to [ $^{125}\text{I}$ ] half-life. Blood volume  
243 was set to 4% of the body weight [38]. Mean values of the injection dose samples  
244 gathered during vaccination were used to determine total cpm recovery (%) at day 1. To  
245 determine the stability of retention, the daily cpm means were related to recovery at day  
246 1. Daily cpm means were used to determine anatomical distribution.

247

#### 248 *2.11 RNA isolation and cDNA synthesis*

249 Tissue samples (20-30 mg) were removed from RNAlater® and homogenized in lysis  
250 buffer from the RNeasy mini kit (Qiagen) using tubes with ceramic beads (Precellys) and  
251 a Precellys® 24 Homogenizer (Bertin Technologies). Parameters were set for 5300 x g x  
252 3 spins, 10 s. Subsequent RNA extractions and on-column purification with the RNase-  
253 Free DNase Set from Qiagen were performed according to manufacturer instructions.

254 RNA was eluted in 50  $\mu$ l RNase-free water and stored at  $-80^{\circ}\text{C}$  until use. RNA  
255 concentration and quality was determined using NanoDrop® (NanoDrop Technologies)  
256 and 1% agarose gel electrophoresis. High quality samples (260/280 ratio  $> 1.9$  and tight  
257 18S/28S bands) were used for cDNA synthesis. Reverse transcription was performed  
258 with the High Capacity RNA-to-cDNA Master-mix from Applied Biosystems in  
259 accordance with manufacturer instructions. Each reaction contained 400 ng RNA in 20  
260  $\mu$ l. Samples were diluted to 80  $\mu$ l with RNase-free water and stored at  $-80^{\circ}\text{C}$ .

261

### 262 *2.12 Quantitative reverse transcription polymerase chain reaction (QPCR)*

263 Quantitative PCR was performed according to manufacturer instructions using Fast  
264 SYBR® Green Master Mix (Applied Biosystems) and primers previously applied in our  
265 laboratory (Table 3). Primer efficiency was determined using a six-point 1:2 dilution  
266 series in triplicate, with an initial cDNA concentration of 20 ng. All primers were free of  
267 primer-dimers in no-template control and showed a single peak in the dissociation curve.  
268 Samples containing 20 ng cDNA were run in triplicate, with each plate including no-  
269 template control and an inter-run calibrator. Analysis was performed on a 7500 Fast Real-  
270 Time PCR System (Applied Biosystems) with the thermal cycler profile set to  $95^{\circ}\text{C}$  for  
271 20 s, 40 cycles of  $95^{\circ}\text{C}$  for 3 s and 40 cycles of  $60^{\circ}\text{C}$  for 30 s. Dissociation curves were  
272 performed on all samples. The 7500 Software Relative Quantification Study Application  
273 (v2.0.4, Applied Biosystems) was used to determine  $C_T$  values, with walking baseline  
274 and threshold set manually to be equal for all genes. Relative gene expression was  
275 determined by the Pfaffl method [39], comparing saline injected fish to treated groups.  
276 To determine relative expression of luciferase the highest day 1 transcript average was

277 used as control. Head kidney and spleen samples from day 2 and 7 were also checked for  
278 luciferase transcripts.

279

### 280 *2.13 Histology*

281 Muscle samples from days 2, 7 and 30 post injection were chosen for histology. The  
282 service of routine histological processing and staining with hematoxylin and eosin (HE)  
283 was purchased from the National Veterinary Institute (Oslo, Norway). Sections were  
284 studied by light microscopy for signs of hemorrhages, tissue degradation and  
285 inflammation. Using the changes in day 2 saline injected fish as a baseline, observed  
286 changes were classified as either moderate (+) or strong (++). Moderate changes were  
287 determined as largely limited to the needle trajectory, with inflammatory cells primarily  
288 associated with degenerated tissue and/or dispersed among intact muscle cells. Strong  
289 changes were seen as degeneration and/or inflammation spreading beyond the needle  
290 trajectory, with few or no intact muscle cells present within the cellular infiltrate. The  
291 histopathology scores were performed as blind testing by two people.

292

### 293 *2.14 Statistical analysis*

294 Microsoft Excel (Microsoft™) was used for arrangement of data as well as calculation of  
295 biodistribution and relative gene expression. Statistical analyses for real-time PCR were  
296 performed with IBM SPSS (Statistical Package for the Social Sciences, version 19.0). All  
297 data were natural log transformed prior to analysis, and normality verified by the  
298 Shapiro-Wilk test. Levene's test of equality of variances was used to check for  
299 homoscedasticity. Homoscedastic data were analyzed by one-way ANOVA with Tukey

300 as the post hoc test. Where homoscedasticity was violated, the Welch test of equality of  
301 means was applied, followed by Dunnett T3 post hoc. Graphs were constructed with  
302 Microsoft Excel and SPSS.

303

304

### 305 **3. Results**

#### 306 *3.1 Particle characterization*

307 The encapsulation efficiency and loading of <sup>125</sup>I-f-pDNA were low for both particles  
308 sizes. The different particle characteristics are summarized in table 1, where empty  
309 particles have been excluded due to minor size differences. The mean size of  
310 nanoparticles was 320 nm by intensity distribution, with more than 90% measuring less  
311 than 500 nm. The number weight mean diameter of microparticles was 3-4 μm, with 80%  
312 measuring less than 5 μm and more than 90% smaller than 10 μm.

313

#### 314 *3.2 In vitro particle stability and pDNA release*

315 Neutral pH and a temperature of 8°C were chosen in order to simulate *in vivo* conditions.  
316 Initial burst release was 81% for NP-(<sup>125</sup>I-f-pDNA) and 49% for MP-(<sup>125</sup>I-f-pDNA). Both  
317 groups subsequently displayed a slow and sustained release, with a 96% and 69 %  
318 accumulated release at day 70 (Fig. 1).

319

#### 320 *3.3 Anatomical distribution and depot of vaccine formulations*

321 No radioactivity was registered in blood later than day 7 post injection. The average total  
322 cpm recovery at day 1 ranged from 15% for NP-(<sup>125</sup>I-f-pDNA) to 39% for <sup>125</sup>I-f-pDNA

323 (results not shown). Radioactivity was primarily recovered from the injection site, organs  
324 and trunk kidney. High degrees of similarities in tissue distribution were observed for  
325 NP-(<sup>125</sup>I-f-pDNA) and <sup>125</sup>I-f-pDNA (Fig. 2A, B). Likewise, MP-(<sup>125</sup>I-f-pDNA) and FIA-  
326 (<sup>125</sup>I-f-pDNA) had similar distribution profiles and injection site depots (Fig. 2C, D). The  
327 trunk kidney was the primary site of recovery for NP-(<sup>125</sup>I-f-pDNA) and <sup>125</sup>I-f-pDNA,  
328 containing almost 80% of total radiation at day 70. NP-(<sup>125</sup>I-f-pDNA) showed higher  
329 injection site retention (5%) at day 70 compared to <sup>125</sup>I-f-pDNA (1%). The respective  
330 values for MP-(<sup>125</sup>I-f-pDNA) and FIA-(<sup>125</sup>I-f-pDNA) were 34% and 26%, with retention  
331 in trunk kidney reaching 32% and 27% at day 70.

332

### 333 *3.4 Quantitative reverse transcription polymerase chain reaction (QPCR)*

#### 334 *3.4.1 Expression of luciferase reporter gene*

335 FIA-(<sup>125</sup>I-f-pDNA) induced the highest luciferase transcript average in muscle at day 1  
336 and was chosen as calibrator for this tissue. FIA-(<sup>125</sup>I-f-pDNA) also induced the highest  
337 individual levels of luciferase transcripts throughout the experiment, with significant  
338 expression at day 1, 4 and 14 ( $p \leq 0.032$ ) (Fig. 3). Naked plasmids consistently induced  
339 higher expression than the particle formulations, with significance for pDNA at day 1-7  
340 ( $p \leq 0.042$ ) and <sup>125</sup>I-f-pDNA at day 4 ( $p = 0.018$ ). No significant differences were found  
341 at days 30 and 70. Low luciferase transcript levels were detected in head kidney, with  
342 pDNA and <sup>125</sup>I-f-pDNA inducing significant expression compared to NP-<sup>125</sup>I-f-pDNA at  
343 day 2 ( $p \leq 0.016$ , results not shown). No expression was detected in the spleen.

344

345

346 *3.4.2 Proinflammatory cytokines IL-1 $\beta$  and TNF- $\alpha$*

347 The particle formulations significantly up-regulated IL-1 $\beta$  in muscle samples at all time-  
348 points; NP-(<sup>125</sup>I-f-pDNA) ( $p \leq 0.002$ ), NP ( $p \leq 0.004$ ), MP-(<sup>125</sup>I-f-pDNA) ( $p \leq 0.003$ ),  
349 MP ( $p \leq 0.015$ ) (Fig. 4A). From day 2 the up-regulation was significant compared to all  
350 non-particle groups. MP formulations consistently induced the highest expression. FIA-  
351 (<sup>125</sup>I-f-pDNA) significantly up-regulated IL-1 $\beta$  in muscle at day 7 ( $p = 0.000$ ). Significant  
352 expression of TNF- $\alpha$  in head kidney was only found at day 4, with NP-(<sup>125</sup>I-f-pDNA) ( $p$   
353  $= 0.034$ ) and MP ( $p = 0.008$ ) (Fig. 4B). No significant expression of TNF- $\alpha$  was found in  
354 the spleen or muscle.

355

356 *3.4.3 IFN- $\alpha$  and Mx*

357 NP-(<sup>125</sup>I-f-pDNA) significantly up-regulated IFN- $\alpha$  at the injection site at day 4 ( $p =$   
358  $0.005$ ). Levels in head kidney were generally low, with significant up-regulation by <sup>125</sup>I-  
359 f-pDNA ( $p = 0.000$ ) at day 2. NP-(<sup>125</sup>I-f-pDNA) ( $p \leq 0.003$ ) and NP ( $p \leq 0.036$ )  
360 significantly up-regulated IFN- $\alpha$  in spleen at day 1 and 2 (results not shown). Levels of  
361 Mx at the injection site increased for all groups from day 1 to 7. NP-(<sup>125</sup>I-f-pDNA)  
362 induced significant expression at day 2-7 ( $p = 0.000$ ), and was superior to all groups at  
363 day 4 and 7 ( $p \leq 0.020$ ). MP-(<sup>125</sup>I-f-pDNA) significantly up-regulated Mx in muscle at  
364 day 2 and 4 ( $p \leq 0.006$ ) (Fig. 5A). NP-(<sup>125</sup>I-f-pDNA) appeared the most potent treatment  
365 for inducing Mx in head kidney, but no significance was found (Fig. 5B). Mx expression  
366 increased in spleen for all groups from day 1 to 7, with significance for NP-(<sup>125</sup>I-f-pDNA)  
367 at day 4 ( $p = 0.013$ ) (Fig. 5C).

368

369 *3.4.4 CD8 and Eomes*

370 There was no significant up-regulation of CD8 in any tissue. Several muscle samples  
371 showed no CD8 expression, and no statistical analyses could therefore be performed.

372 No expression of CD8 could be detected at day 2 in head kidney samples from fish  
373 injected with <sup>125</sup>I-f-pDNA. Interestingly, these samples induced the only significant up-  
374 regulation of Eomes observed within any tissue ( $p = 0.000$ ) (results not shown).

375

376 *3.6 Histopathology*

377 Tissue sections of injection site samples were examined by light microscopy for signs of  
378 hemorrhages, muscle degeneration and inflammation (Table 4). PBS caused only minor  
379 hemorrhages and tissue degeneration at day 2 (Fig. 6A), indicating that later changes  
380 were likely the results of the different treatments. Hemorrhages were most pronounced at  
381 day 2 in all groups. Administration of PBS and <sup>125</sup>I-f-pDNA caused moderate muscle  
382 degeneration, but no inflammation. Both tissue degeneration and inflammation were  
383 observed for pDNA (Fig. 6C), but both pathologies were more frequent with particles  
384 formulations. MP-(<sup>125</sup>I-f-pDNA) and FIA-(<sup>125</sup>I-f-pDNA) both demonstrated strong  
385 inflammation at day 30 (Fig. 6B, D), with a high influx of inflammatory cells that for  
386 FIA-(<sup>125</sup>I-f-pDNA) was concentrated around possible oil-droplets. The histopathological  
387 changes caused by particles seemed to depend on particle size (nano vs. micro) rather  
388 than content (empty vs. pDNA).

389

390

391

#### 392 4. Discussion

393 The use of PLGA particle constructs as carriers for DNA vaccine delivery has so far  
394 received little attention in fish studies [1, 40]. We have investigated distribution/depot,  
395 transgene and immune gene transcription as well as injection site histopathology  
396 following intramuscular injection of Atlantic salmon with PLGA particles carrying  
397 pDNA encoding luciferase. The double emulsion solvent evaporation method [2, 37] was  
398 used to prepare nano- and microparticles with mean diameters of 320 nm and 4  $\mu$ m,  
399 respectively. Low pDNA encapsulation appears to be a recurring problem, and our results  
400 (<30% for both particle sizes) are supported by other studies [12, 35].

401 One of the challenges of conventional DNA vaccination is the rapid tissue  
402 clearance and on-site degradation of DNA, which may result in reduced pDNA uptake  
403 and transgene expression [8, 10]. **Although oil adjuvants are not commonly applied for**  
404 **intramuscular vaccine delivery, FIA-(<sup>125</sup>I-f-pDNA) provided a positive control to**  
405 **measure the depot potential of nano- and microparticles.** The high burst release observed  
406 for NP-(<sup>125</sup>I-f-pDNA) during the *in vitro* release study (Fig. 1) likely explains the strong  
407 similarities between this group and <sup>125</sup>I-f-pDNA (Fig. 2A, B), a similarity reflected also  
408 in the injection site histopathology (Table 4). In comparison, the injection site retention  
409 of MP-(<sup>125</sup>I-f-pDNA) remained similar to that of FIA-(<sup>125</sup>I-f-pDNA) throughout the study  
410 (Fig. 2C, D). The duration of the MP-(<sup>125</sup>I-f-pDNA) and FIA-(<sup>125</sup>I-f-pDNA) depots likely  
411 contributed to the severe histopathological inflammations observed in tissue sections  
412 from both groups at day 30 (Fig. 6B, D). **The transfection of infiltrating cells has been**  
413 **shown to take place in both fish and mammals [35, 37, 41], and transient inflammatory**  
414 **responses may thus contribute to increased transgene expression. Long lasting**



415 inflammations such as seen with MP-(<sup>125</sup>I-f-pDNA) and FIA-(<sup>125</sup>I-f-pDNA) are, however,  
416 undesirable in a product meant for consumption. It would appear that nanoparticles may  
417 be favorable in order to avoid potential tissue damage, but the small sample sizes meant  
418 we could only obtain an indication of the histopathological influence of the various  
419 treatments.

420 Although the similarities in injection site retention were not reflected in the  
421 expression of the luciferase transgene (Fig. 3), the observation that FIA-(<sup>125</sup>I-f-pDNA)  
422 induced the highest individual levels of luciferase transcripts suggests that increased  
423 cellular infiltration along with a high injection site pDNA depot may be of benefit to  
424 transgene expression in Atlantic salmon. The significantly lower expression obtained  
425 with encapsulated pDNA could be a result of the preparation conditions, as the W<sub>1</sub>/O/W<sub>2</sub>  
426 method has been shown to cause a partial reduction in the content of supercoiled (SC)  
427 DNA topofrom that contributes to a lower transfection efficiency [1, 8, 37, 42]. The  
428 process of emulsification required lower shear forces and shorter duration of preparation  
429 and may thus have preserved a larger portion of SC DNA in FIA-(<sup>125</sup>I-f-pDNA). We did  
430 not, however, address whether the encapsulation of <sup>125</sup>I-f-pDNA resulted in an altered SC  
431 content. The absence of significant differences in luciferase expression at day 30 and 70  
432 still indicated a certain level of stability in particle groups that could result from a  
433 continued release of bioactive pDNA even at later time-points.

434 Another explanation for the low transcription levels obtained with encapsulated  
435 pDNA-Luc may lie with the inflammatory cytokine responses. Induced not only by  
436 stimulation of PRRs but also by PLGA itself [43, 44], IL-1 $\beta$  and TNF- $\alpha$  have both  
437 demonstrated inhibitory effects on transgene expression even at low concentrations,

438 contributing to a reduced transfection efficiency of encapsulated DNA *in vivo* as opposed  
439 to *in vitro* [2, 37, 45]. The nano- and microparticle formulations significantly up-  
440 regulated IL-1 $\beta$  at the injection site at all time-points (Fig. 4A), and while the expression  
441 of TNF- $\alpha$  was generally low a synergistic effect of different cytokines on the inhibition of  
442 transgene expression has been reported [45]. **In comparison, the levels of IL-1 $\beta$  in fish**  
443 **injected with FIA-(<sup>125</sup>I-f-pDNA) were not found significant until 7 days post**  
444 **administration, indicating that PLGA may provide a more potent inflammatory stimulus**  
445 **than the oil adjuvant even in the absence of pronounced inflammatory histopathology.**

446 **Viral challenge studies in fish have shown that specific protection may be**  
447 **acquired even with very low doses of DNA, and innate antiviral responses also appear to**  
448 **play a more critical role in fish than mammals upon exposure to viruses [46, 47].**  
449 Whereas luciferase is unlikely to induce a differentiation of antigen specific CD8<sup>+</sup> T-cells  
450 due to low immunogenicity in *in vivo* studies [48, 49], type I IFNs play an important role  
451 in the clonal expansion of CD8<sup>+</sup> T-cells and may enhance CTL responses when  
452 immunogenic transgene products are expressed [29]. Whereas the expression of IFN- $\alpha$   
453 was generally low and transient, NP-(<sup>125</sup>I-f-pDNA) still appeared the most potent inducer  
454 of antiviral responses and significantly up-regulated the expression of Mx in all tissues  
455 (Fig. 5). This result supports a previous study on the influence of particle size on the  
456 cytokine profile induced after administration of particle associated CpG DNA [50]. We  
457 did observe that formulations with naked pDNA significantly up-regulated both Eomes  
458 and IFN- $\alpha$  in head kidney at day 2, but no statistical correlation between these genes was  
459 found for any other group, tissue or time-point.

460 This study is the first on intramuscular injection of Atlantic salmon with PLGA  
461 particles carrying pDNA. Our particle formulations did not induce transgene expression  
462 as efficiently as injection of naked plasmids, but appeared to provide a continued release  
463 of bioactive pDNA even at the end of the study. A strong expression of transgene may  
464 not always be necessary in order to mount a significantly protective immune response,  
465 and an efficient up-regulation of innate antiviral responses in particular might enhance  
466 the immunogenicity of an antiviral vaccine. Both particle sizes proved superior to naked  
467 pDNA injection for the induction of IL-1 $\beta$  as well as an influx of inflammatory cells at  
468 the injection site, but only encapsulation into nanoparticles significantly increased the  
469 expression of IFN- $\alpha$  and Mx. Together these results indicate that PLGA nanoparticles as  
470 carriers for plasmid vectors encoding viral antigens might enhance the responses to DNA  
471 vaccines.

472

473

#### 474 **Acknowledgements**

475 This project was funded by the Research Council of Norway (project nos. 182035 and  
476 183204/S40) and Tromsø Research Foundation (“Induction and assessment of T cell  
477 immunity to virus antigens in salmonids). The authors would also like to acknowledge  
478 Merete Skar for technical help during particle sizing and Bjarte Lund for his assistance  
479 with RNA isolation.

480

481

482

- 483 1. Tian J, Yu J. Poly(lactic-co-glycolic acid) nanoparticles as candidate DNA  
484 vaccine carrier for oral immunization of Japanese flounder (*Paralichthys*  
485 *olivaceus*) against lymphocystis disease virus. *Fish Shellfish Immunol*  
486 2011;30:109-17.
- 487 2. Cohen H, Levy RJ, Gao J, Fishbein I, Kousaev V, Sosnowski S, et al. Sustained  
488 delivery and expression of DNA encapsulated in polymeric nanoparticles. *Gene*  
489 *Ther* 2000;7:1896-905.
- 490 3. Semete B, Booyesen L, Lemmer Y, Kalombo L, Katata L, Verschoor J, et al. *In*  
491 *vivo* evaluation of the biodistribution and safety of PLGA nanoparticles as drug  
492 delivery systems. *Nanomed Nanotechnol* 2010;6:662-71.
- 493 4. Newman KD, Elamanchili P, Kwon GS, Samuel J. Uptake of poly(D,L-lactic-co-  
494 glycolic acid) microspheres by antigen-presenting cells *in vivo*. *J Biomed Mater*  
495 *Res* 2002;60:480-6.
- 496 5. Fredriksen BN, Sævareid K, McAuley L, Lane ME, Bøggwald J, Dalmo RA. Early  
497 immune responses in Atlantic salmon (*Salmo salar* L.) after immunization with  
498 PLGA nanoparticles loaded with a model antigen and  $\beta$ -glucan. *Vaccine*  
499 2011;29:8338-49.
- 500 6. Panyam J, Zhou WZ, Prabha S, Sahoo SK, Labhasetwar V. Rapid endo-lysosomal  
501 escape of poly(DL-lactide-co-glycolide) nanoparticles: implications for drug and  
502 gene delivery. *FASEB J* 2002;16:1217-26.
- 503 7. Schlosser E, Mueller M, Fischer S, Basta S, Busch DH, Gander B, et al. TLR  
504 ligands and antigen need to be coencapsulated into the same biodegradable  
505 microsphere for the generation of potent cytotoxic T lymphocyte responses.  
506 *Vaccine* 2008;26:1626-37.
- 507 8. Manthorpe M, Cornefertjensen F, Hartikka J, Felgner J, Rundell A, Margalith M,  
508 et al. Gene-therapy by intramuscular injection of plasmid DNA - studies on firefly  
509 luciferase gene-expression in mice. *Hum Gene Ther* 1993;4:419-31.
- 510 9. Garver K, Conway C, Elliott D, Kurath G. Analysis of DNA-vaccinated fish  
511 reveals viral antigen in muscle, kidney and thymus, and transient histopathologic  
512 changes. *J Mar Biotechnol* 2005;7:540-53.
- 513 10. Tonheim TC, Dalmo RA, Bøggwald J, Seternes T. Specific uptake of plasmid  
514 DNA without reporter gene expression in Atlantic salmon (*Salmo salar* L.) kidney  
515 after intramuscular administration. *Fish Shellfish Immunol* 2008;24:90-101.
- 516 11. Prabha S, Labhasetwar V. Critical determinants in PLGA/PLA nanoparticle-  
517 mediated gene expression. *Pharm Res* 2004;21:354-64.
- 518 12. Diez S, Tros de Ilarduya C. Versatility of biodegradable poly(D,L-lactic-co-  
519 glycolic acid) microspheres for plasmid DNA delivery. *Eur J Pharm Biopharm*  
520 2006;63:188-97.
- 521 13. Shen H, Ackerman AL, Cody V, Giodini A, Hinson ER, Cresswell P, et al.  
522 Enhanced and prolonged cross-presentation following endosomal escape of  
523 exogenous antigens encapsulated in biodegradable nanoparticles. *Immunology*  
524 2006;117:78-88.
- 525 14. Rejman J, Oberle V, Zuhorn IS, Hoekstra D. Size-dependent internalization of  
526 particles via the pathways of clathrin- and caveolae-mediated endocytosis.  
527 *Biochem J* 2004;377:159-69.

- 528 15. Satkauskas S, Bureau MF, Mahfoudi A, Mir LM. Slow accumulation of plasmid  
529 in muscle cells: Supporting evidence for a mechanism of DNA uptake by  
530 receptor-mediated endocytosis. *Mol Ther* 2001;4:317-23.
- 531 16. Krieg AM, Yi A-K, Matson S, Waldschmidt TJ, Bishop GA, Teasdale R, et al.  
532 CpG motifs in bacterial DNA trigger direct B-cell activation. *Nature*  
533 1995;374:546-9.
- 534 17. Utke K, Kock H, Schuetze H, Bergmann SM, Lorenzen N, Einer-Jensen K, et al.  
535 Cell-mediated immune responses in rainbow trout after DNA immunization  
536 against the viral hemorrhagic septicemia virus. *Dev Comp Immunol* 2008;32:239-  
537 52.
- 538 18. Klinman DM, Yamshchikov G, Ishigatsubo Y. Contribution of CpG motifs to the  
539 immunogenicity of DNA vaccines. *J Immunol* 1997;158:3635-9.
- 540 19. Shimizu Y, Newman W, Tanaka Y, Shaw S. Lymphocyte interactions with  
541 endothelial cells. *Immunol Today* 1992;13:106-12.
- 542 20. Mathew JA, Guo YX, Goh KP, Chan J, Verburg-van Kemenade BML, Kwang J.  
543 Characterisation of a monoclonal antibody to carp IL-1 $\beta$  and the development of a  
544 sensitive capture ELISA. *Fish Shellfish Immunol* 2002;13:85-95.
- 545 21. Zou J, Peddie S, Scapigliati G, Zhang Y, Bols NC, Ellis AE, et al. Functional  
546 characterisation of the recombinant tumor necrosis factors in rainbow trout,  
547 *Oncorhynchus mykiss*. *Dev Comp Immunol* 2003;27:813-22.
- 548 22. Zhang A, Chen D, Wei H, Du L, Zhao T, Wang X, et al. Functional  
549 characterization of TNF- $\alpha$  in grass carp head kidney leukocytes: Induction and  
550 involvement in the regulation of NF- $\kappa$ B signaling. *Fish Shellfish Immunol*  
551 2012;33:1123-32.
- 552 23. Latz E, Schoenemeyer A, Visintin A, Fitzgerald KA, Monks BG, Knetter CF, et  
553 al. TLR9 signals after translocating from the ER to CpG DNA in the lysosome.  
554 *Nat Immunol* 2004;5:190-8.
- 555 24. Hemmi H, Takeuchi O, Kawai T, Kaisho T, Sato S, Sanjo H, et al. A Toll-like  
556 receptor recognizes bacterial DNA. *Nature* 2000;408:740-5.
- 557 25. Whyte SK. The innate immune response of finfish – A review of current  
558 knowledge. *Fish Shellfish Immunol* 2007;23:1127-51.
- 559 26. Nygaard R, Husgard S, Sommer A-I, Leong J-AC, Robertsen B. Induction of Mx  
560 protein by interferon and double-stranded RNA in salmonid cells. *Fish Shellfish*  
561 *Immunol* 2000;10:435-50.
- 562 27. Larsen R, Rokenes TP, Robertsen B. Inhibition of infectious pancreatic necrosis  
563 virus replication by Atlantic salmon Mx1 protein. *J Virol* 2004;78:7938-44.
- 564 28. Horisberger MA, De Staritzky K. Expression and stability of the Mx protein in  
565 different tissues of mice, in response to interferon inducers or to influenza virus  
566 infection. *J Interferon Res* 1989;9:583-90.
- 567 29. Marshall HD, Prince AL, Berg LJ, Welsh RM. IFN- $\alpha\beta$  and self-MHC divert CD8  
568 T cells into a distinct differentiation pathway characterized by rapid acquisition of  
569 effector functions. *J Immunol* 2010;185:1419-28.
- 570 30. Moore LJ, Somamoto T, Lie KK, Dijkstra JM, Hordvik I. Characterisation of  
571 salmon and trout CD8 $\alpha$  and CD8 $\beta$ . *Mol Immunol* 2005;42:1225-34.

- 572 31. Takizawa F, Dijkstra JM, Kotterba P, Korytář T, Kock H, Köllner B, et al. The  
573 expression of CD8 $\alpha$  discriminates distinct T cell subsets in teleost fish. *Dev Comp*  
574 *Immunol* 2011;35:752-63.
- 575 32. Intlekofer AM, Takemoto N, Wherry EJ, Longworth SA, Northrup JT, Palanivel  
576 VR, et al. Effector and memory CD8<sup>+</sup> T cell fate coupled by T-bet and  
577 Eomesodermin. *Nat Immunol* 2005;6:1236-44.
- 578 33. Pearce EL, Mullen AC, Martins GA, Krawczyk CM, Hutchins AS, Zediak VP, et  
579 al. Control of effector CD8<sup>+</sup> T cell function by the transcription factor  
580 Eomesodermin. *Science* 2003;302:1041-3.
- 581 34. Kumari J, Bogwald J, Dalmo RA. Eomesodermin of Atlantic salmon: An  
582 important regulator of cytolytic gene and interferon gamma expression in spleen  
583 lymphocytes. *PLoS One* 2013;8:e55893.
- 584 35. Jang JH, Shea LD. Intramuscular delivery of DNA releasing microspheres:  
585 Microsphere properties and transgene expression. *J Control Release*  
586 2006;112:120-8.
- 587 36. Piatyszek MA, Jarmolowski A, Augustyniak J. Iodo-Gen-mediated  
588 radioiodination of nucleic acids. *Anal Biochem* 1988;172:356-9.
- 589 37. Labhasetwar V, Bonadio J, Goldstein SA, Levy JR. Gene transfection using  
590 biodegradable nanospheres: results in tissue culture and a rat osteotomy model.  
591 *Colloids Surf, B* 1999;16:281-90.
- 592 38. Ferguson H. Systemic pathology of fish: a text and atlas of comparative tissue  
593 responses in disease of teleosts. 1st ed: Ames: Iowa State University Press; 1989.
- 594 39. Pfaffl MW. A new mathematical model for relative quantification in real-time  
595 RT-PCR. *Nucleic Acids Res* 2001;29:e45.
- 596 40. Adomako M, St-Hilaire S, Zheng Y, Eley J, Marcum RD, Sealey W, et al. Oral  
597 DNA vaccination of rainbow trout, *Oncorhynchus mykiss* (Walbaum), against  
598 infectious haematopoietic necrosis virus using PLGA [Poly(D,L-Lactic-Co-  
599 Glycolic Acid)] nanoparticles. *J Fish Dis* 2012;35:203-14.
- 600 41. Boudinot P, Blanco M, de Kinkelin P, Benmansour A. Combined DNA  
601 immunization with the glycoprotein gene of viral hemorrhagic septicemia virus  
602 and infectious hematopoietic necrosis virus induces double-specific protective  
603 immunity and nonspecific response in rainbow trout. *Virology* 1998;249:297-306.
- 604 42. Weintraub H, Cheng PF, Conrad K. Expression of transfected DNA depends on  
605 DNA topology. *Cell* 1986;46:115-22.
- 606 43. Ding T, Sun J, Zhang P. Immune evaluation of biomaterials in TNF- $\alpha$  and IL-1 $\beta$   
607 at mRNA level. *J Mater Sci Mater Med* 2007;18:2233-6.
- 608 44. Sharp FA, Ruane D, Claass B, Creagh E, Harris J, Malyala P, et al. Uptake of  
609 particulate vaccine adjuvants by dendritic cells activates the NALP3  
610 inflammasome. *PNAS* 2009;106:870-5.
- 611 45. Tan Y, Li S, Pitt BR, Huang L. The inhibitory role of CpG immunostimulatory  
612 motifs in cationic lipid vector-mediated transgene expression *in vivo*. *Hum Gene*  
613 *Ther* 1999;10:2153-61.
- 614 46. McLauchlan PE, Collet B, Ingerslev E, Secombes CJ, Lorenzen N, Ellis AE.  
615 DNA vaccination against viral haemorrhagic septicaemia (VHS) in rainbow trout:  
616 size, dose, route of injection and duration of protection—early protection  
617 correlates with Mx expression. *Fish Shellfish Immunol* 2003;15:39-50.

- 618 47. Garver KA, LaPatra SE, Kurath G. Efficacy of an infectious hematopoietic  
619 necrosis (IHN) virus DNA vaccine in Chinook *Oncorhynchus tshawytscha* and  
620 sockeye *O. nerka* salmon. *Dis Aquat Org* 2005;64:13-22.
- 621 48. Wolff J, Malone R, Williams P, Chong W, Acsadi G, Jani A, et al. Direct gene  
622 transfer into mouse muscle *in vivo*. *Science* 1990;247:1465-8.
- 623 49. Heppell J, Lorenzen N, Armstrong NK, Wu T, Lorenzen E, Einer-Jensen K, et al.  
624 Development of DNA vaccines for fish: vector design, intramuscular injection  
625 and antigen expression using viral haemorrhagic septicaemia virus genes as  
626 model. *Fish Shellfish Immunol* 1998;8:271-86.
- 627 50. Chen HC, Sun B, Tran KK, Shen H. Effects of particle size on toll-like receptor  
628 9-mediated cytokine profiles. *Biomaterials* 2011;32:1731-7.
- 629  
630

**Ref. No.: FSIM-D-12-00522**

**Response to review of manuscript with title “Transgene and immune gene expression following intramuscular injection of Atlantic salmon (*Salmo salar* L.) with DNA-releasing PLGA nano- and microparticles”.**

**General comments on the revised manuscript:**

For this re-submission revisions have been confined to the introduction and discussion sections of the manuscript, in addition to some figure revisions in response to reviewer’s queries. As the study was not designed to evaluate DNA vaccine efficacy but rather the potential influence of various factors on the expression of a reporter gene, we found it right not to make too much speculation as to how our results might transfer to an actual DNA vaccine trial. An effort has instead been made to clarify the various results and observations in terms of their potential impact – positive or negative – on the expression of the reporter gene.

New additions as well as altered sections of the text have been highlighted in red for easier recognition, and line-references have also been provided in the answers to reviewer queries following below.



**Query 1:**

*In the abstract there are several “pDNA”. The authors should clarify what “p” stands for in the first one.*

Clarification has been made in line (L) 28.

**Query 2:**

*The authors have used a luciferase gene as a reporter gene in the present study. If the authors have been tried a luciferase assay in this project, the authors should show the results of the assay. If not, the author should describe the reason why a luciferase gene has been chosen as a reporter gene.*

No luciferase assay was included in the current project. Luciferase (Luc) was still chosen as it is one of the most common reporter genes and has frequently been applied for the evaluation of transgene expression in fish at both protein and transcription level (L77-79). The application of a Luc-gene hence makes it easier to evaluate and relate the work performed for this manuscript to previously published studies.

**Query 3:**

*In the results of histopathology, it is difficult to understand the histological differences between treated samples and controls for those who are not familiar with the inflamed tissue.*

*a) Please describe the detailed features of muscle degeneration and inflammation in the manuscript or figure legend.*

More detailed descriptions of the various histopathological features including muscle cell degeneration and inflammation have been provided in the figure legend.

*b) Please add the enlarged figures for the inflammatory cells and add the description of the detailed features for the inflammatory cells in fig 6D.*

Detailed features, such as cell types, cannot be provided for the observed inflammatory cells as no immunohistochemical assays were conducted to verify their specific nature. A higher magnification micrograph has been provided for one of the original, lower magnification sections to show the high variation in infiltrating cells.

c) Please add scale bars for the panels in histological figures.

Scale bars have been added.

**Query 4:**

*Although several homolog genes were used as markers for pro-inflammatory, antiviral response and cytotoxic T-cell markers in the present study, the authors should show some proofs that those genes had similar roles in Atlantic salmon by the referring of previous other work, or other way.*

The introduction has been altered to include specific references to studies on function and/or presence of the various cytokines and markers in fish species. For TNF- $\alpha$  and IL-1 $\beta$  the additions can be found in L95-99. Studies on the activities of IFN- $\alpha$  and Mx in teleosts were referenced in the previous draft. Descriptions are now given in L100-106. Brief references to the existence and activity of CD8 in fish have also been made (L106-108), while reference to a very recent study on the expression and function of Eomesodermin in Atlantic salmon has been included in L108-111-

**Query 5:**

*The authors should add the evidence-based descriptions that the early response (1-7 days post vaccination) of immune-related genes showed in the fig. 4 and 5 would be of benefit to DNA vaccination in the discussion part.*

Whereas some mention had been made to the benefit of these early responses, we agree that the original manuscript did not clarify the findings and evaluations of these in a satisfactory manner. The discussion has therefore to some extent been rewritten to clarify potential benefits *as well as* negative effects of the various early immune responses.

The role of proinflammatory cytokines in the migration of inflammatory cells to the site of injection has been specified in the description of biological function (L95-97), whereas the potential influence of these cytokines on DNA vaccines and transgene expression is described in L434-442. Likewise, the antiviral functions of IFN- $\alpha$  and Mx and the relation to CD8 and Eomes expression can be found in the introduction, as described for query 4. In the discussion, L448-449 and L451-453 reference the importance of innate antiviral responses in teleosts and presents the potential benefit to later, acquired

responses. In L455-457 a reference is given to the potential influence of PLGA particle size on the resulting antiviral response.

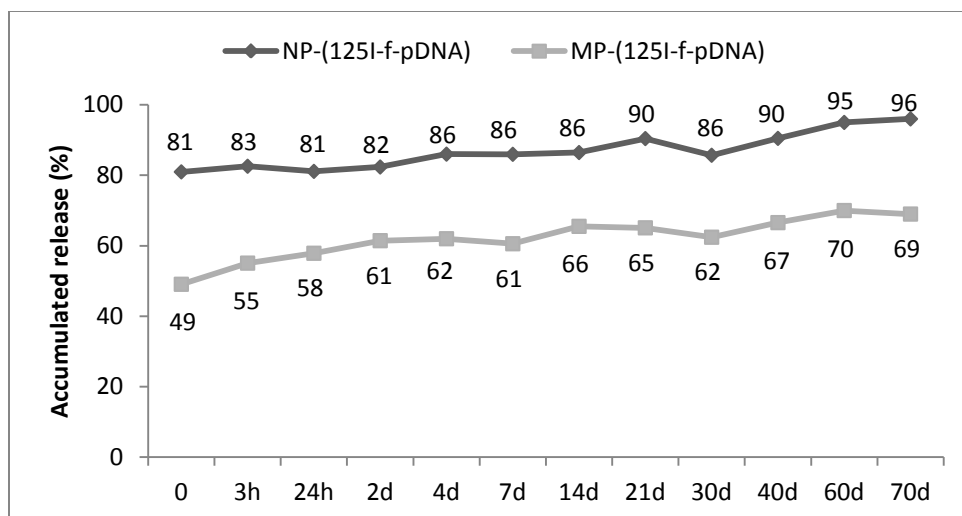


Figure 1 - Release of <sup>125</sup>I-f-pDNA from nano- and microparticles through 70 days of incubation at 8° C, presented as the mean accumulated release (%) of five samples at each time-point.

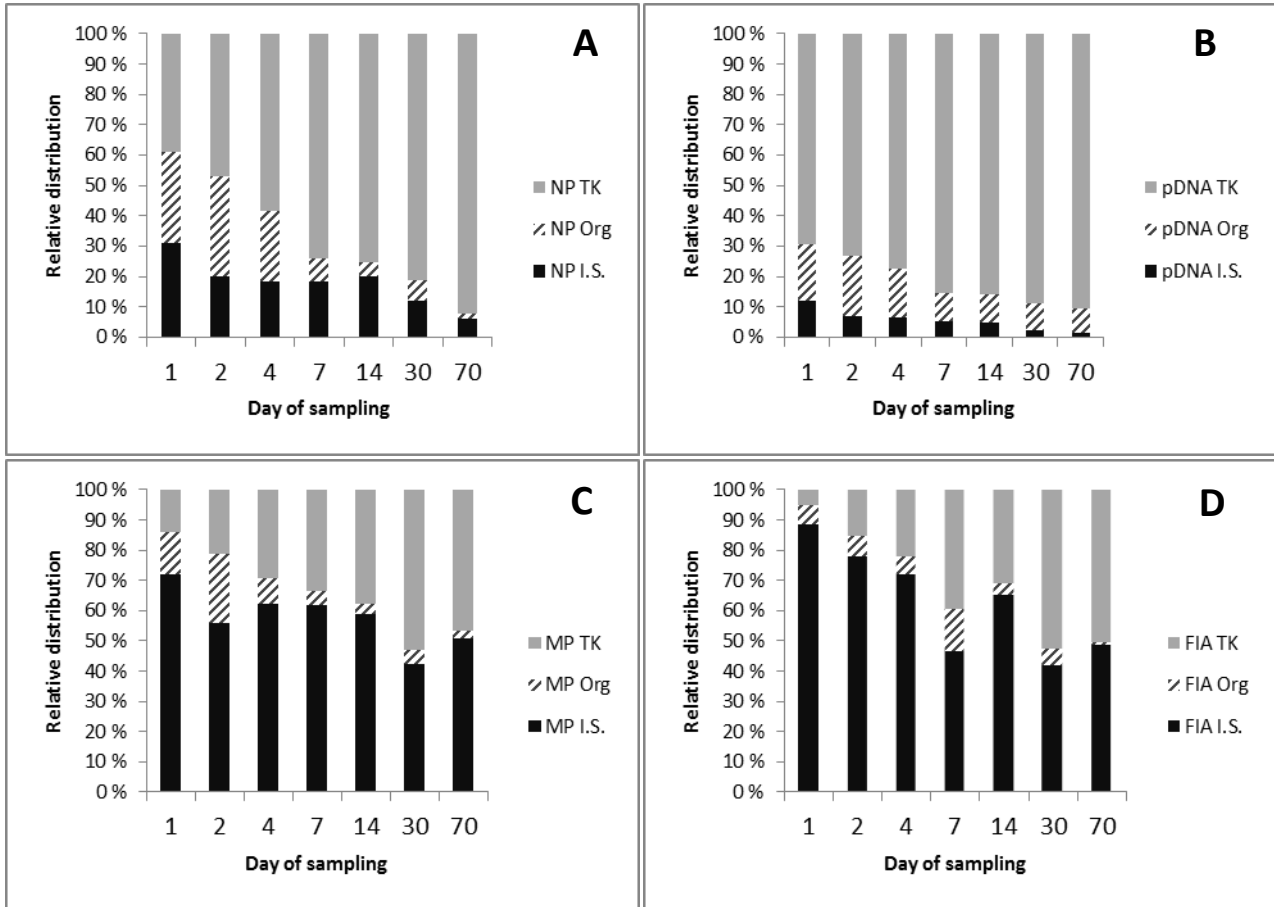


Figure 2 – Radioactivity recovered from samples of trunk kidney (TK), organs (Org) and injection site (I.S.). The stacked bars represent the relative distribution of pDNA among these organs in groups A) NP-(<sup>125</sup>I-f-pDNA), B) <sup>125</sup>I-f-pDNA, C) MP-(<sup>125</sup>I-f-pDNA) and D) FIA-(<sup>125</sup>I-f-pDNA). Five fish were sampled at each time-point.

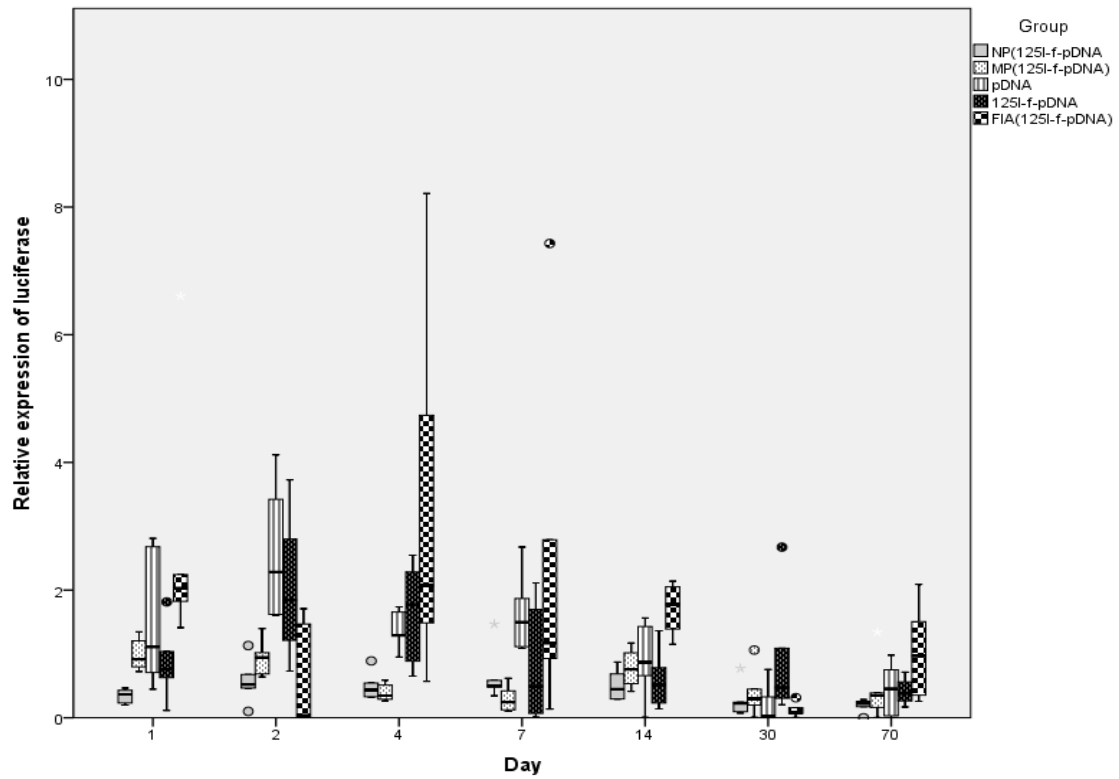


Figure 3 - Relative expression of luciferase mRNA transcripts in muscle from the injection site through the 70 day sample period. The box-plot shows the median value (line) and maximum and minimum values (whiskers), with the box representing 50% of the samples. Circles show outliers. The highest cpm-average at day 1 was found in group FIA-(<sup>125</sup>I-f-pDNA) and was set as calibrator. Six fish were sampled and analyzed at each time-point.

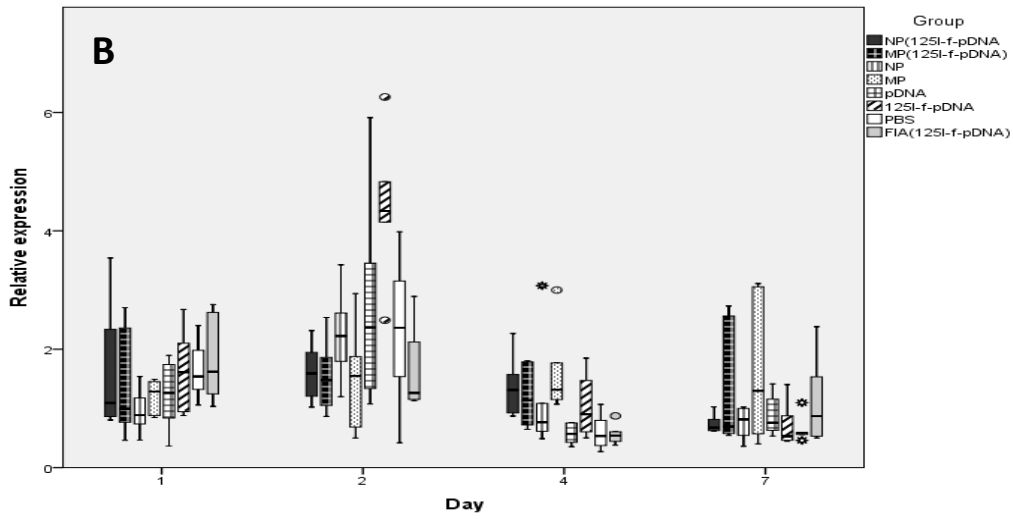
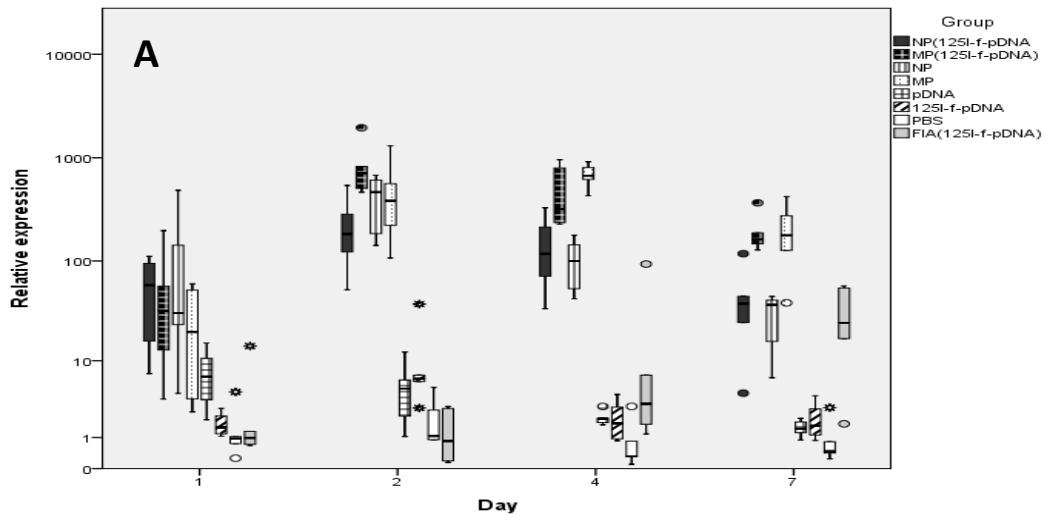


Figure 4 – Relative expression of proinflammatory cytokines; A) IL-1 $\beta$  in muscle from the injection site and B) TNF- $\alpha$  in head kidney. The box-plot shows the median value (line) and maximum and minimum values (whiskers), with the box representing 50% of the samples. Circles show outliers, and asterisks (\*) extreme outliers. Six fish were sampled and analyzed at each time-point.

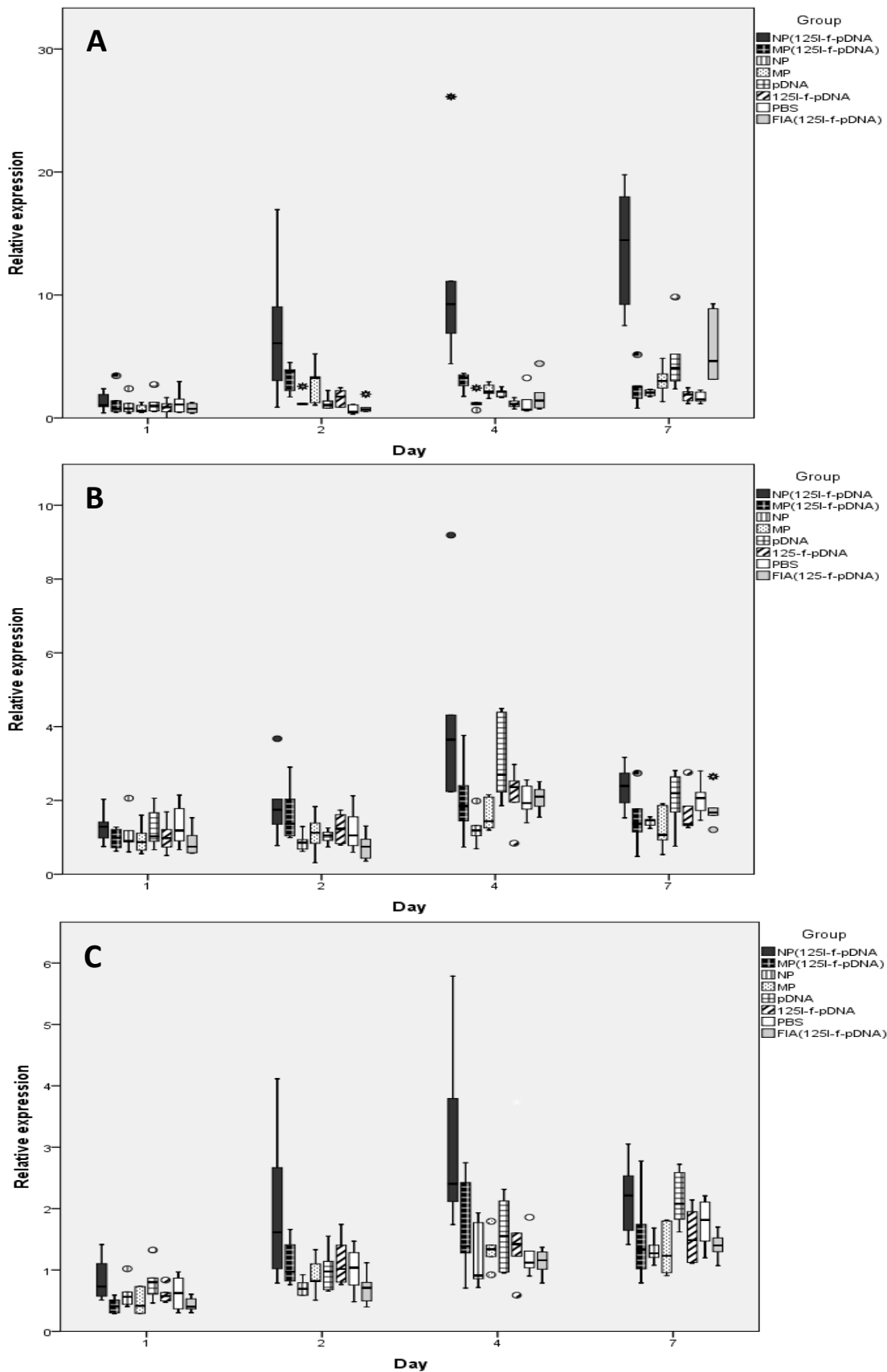
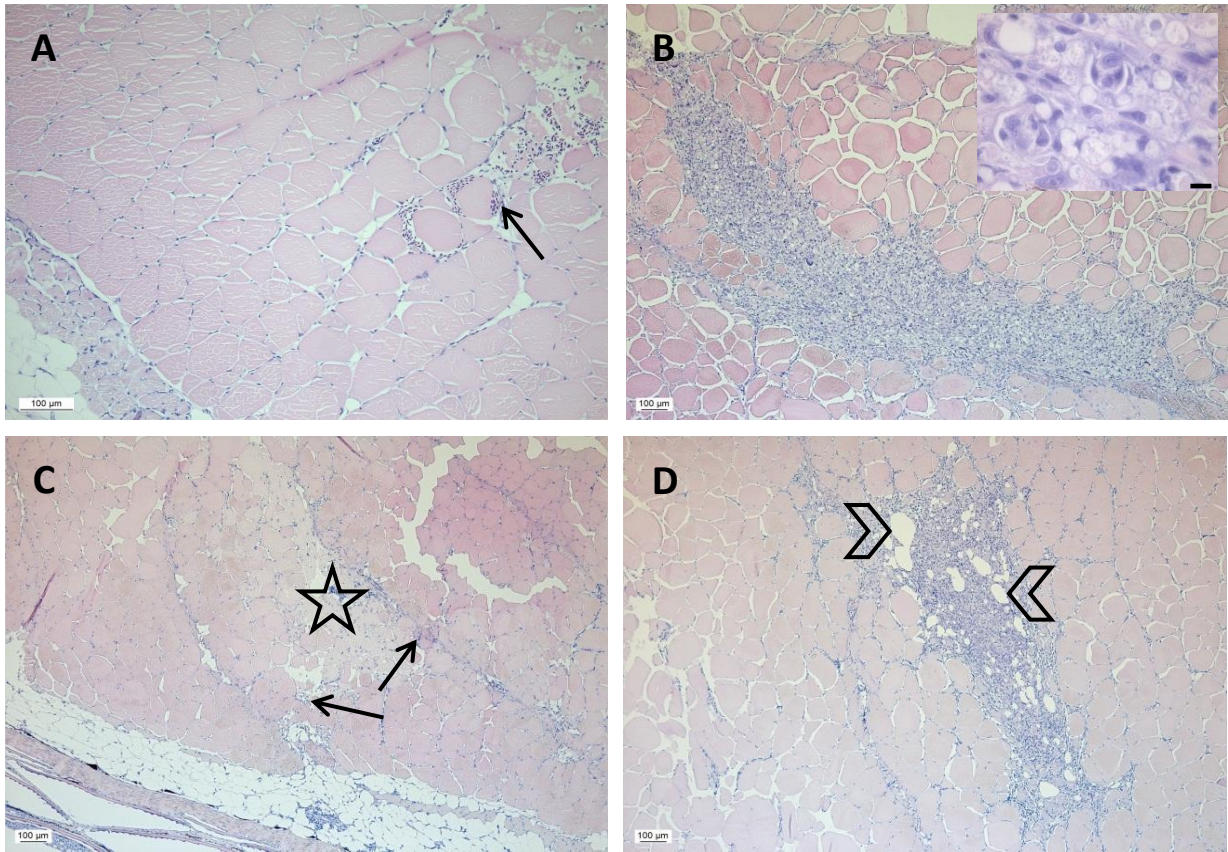


Figure 5 - Expression of the antiviral protein Mx in A) injection site muscle, B) head kidney and C) spleen. The box-plots show median values (line) and maximum and minimum values (whiskers), with the boxes representing 50% of the samples. Circles show outliers, and asterisks (\*) extreme outliers. Six fish were sampled and analyzed at each time-point.





**Figure 6** – All pictures show transversal sections of skeletal muscle from the injection site, stained with hematoxylin and eosin (HE). A) Minor hemorrhages (arrow) and muscle cell degeneration in negative control (PBS) group observed at day 2. B) Massive cellular infiltrate in the myocyte fibre and surrounding interstitium at day 30 in tissue of fish injected with MP-<sup>(125I)-f</sup>-pDNA). Magnification of cellular infiltrate is shown with a 10.0 µm scale-bar. C) Focal muscle cell degeneration (star) and minor hemorrhages (arrows) can be seen at day 7 in samples from fish injected with pDNA. D) Large oil-droplets (arrowheads) surrounded by degenerative muscle fibers and inflammatory cells at day 30 after injection of FIA-<sup>(125I)-f</sup>-pDNA).

**COVER LETTER - Ref. No.: FSIM-D-12-00522**

We are pleased to have the referees' comments, and we have now undertaken the revision that hopefully fulfills the requirements to get the manuscript accepted.

In general, we have met the criticisms made by the referees, and performed the revision accordingly. In addition we have made some minor additional improvements based on new input by the authors. Please note that there are two corresponding authors.

Best wishes,  
Roy A. Dalmo

**Ref. No.: FSIM-D-12-00522**

**Response to review of manuscript with title “Transgene and immune gene expression following intramuscular injection of Atlantic salmon (*Salmo salar* L.) with DNA-releasing PLGA nano- and microparticles”.**

**General comments on the revised manuscript:**

For this re-submission revisions have been confined to the introduction and discussion sections of the manuscript, in addition to some figure revisions in response to reviewer’s queries. As the study was not designed to evaluate DNA vaccine efficacy but rather the potential influence of various factors on the expression of a reporter gene, we found it right not to make too much speculation as to how our results might transfer to an actual DNA vaccine trial. An effort has instead been made to clarify the various results and observations in terms of their potential impact – positive or negative – on the expression of the reporter gene.

New additions as well as altered sections of the text have been highlighted in red and yellow for easier recognition, and line-references have also been provided in the answers to reviewer queries following below.

**Query 1:**

*In the abstract there are several “pDNA”. The authors should clarify what “p” stands for in the first one.*

Clarification has been made in line (L) 28.

**Query 2:**

*The authors have used a luciferase gene as a reporter gene in the present study. If the authors have been tried a luciferase assay in this project, the authors should show the results of the assay. If not, the author should describe the reason why a luciferase gene has been chosen as a reporter gene.*

No luciferase assay was included in the current project. Luciferase (Luc) was still chosen as it is one of the most common reporter genes and has frequently been applied for the evaluation of transgene expression in fish at both protein and transcription level (L77-79). The application of a Luc-gene hence makes it easier to evaluate and relate the work performed for this manuscript to previously published studies.

**Query 3:**

*In the results of histopathology, it is difficult to understand the histological differences between treated samples and controls for those who are not familiar with the inflamed tissue.*

*a) Please describe the detailed features of muscle degeneration and inflammation in the manuscript or figure legend.*

More detailed descriptions of the various histopathological features including muscle cell degeneration and inflammation have been provided in the figure legend.

*b) Please add the enlarged figures for the inflammatory cells and add the description of the detailed features for the inflammatory cells in fig 6D.*

Detailed features, such as cell types, cannot be provided for the observed inflammatory cells as no immunohistochemical assays were conducted to verify their specific nature. A higher magnification micrograph has been inserted for one of the originals (6B) to show the high variation in infiltrating cells.

c) *Please add scale bars for the panels in histological figures.*

Scale bars have been added.

**Query 4:**

*Although several homolog genes were used as markers for pro-inflammatory, antiviral response and cytotoxic T-cell markers in the present study, the authors should show some proofs that those genes had similar roles in Atlantic salmon by the referring of previous other work, or other way.*

The introduction has been revised accordingly to include specific references to studies on function and/or presence of the various cytokines and markers in fish species. For TNF- $\alpha$  and IL-1 $\beta$  the additions can be found in L95-99. Studies on the activities of IFN- $\alpha$  and Mx in teleosts were referenced in the original manuscript. Descriptions are now given in L100-106. Brief references to the existence and activity of CD8 in fish have also been made (L106-108), while reference to a very recent study on the expression and function of Eomesodermin in Atlantic salmon has been included in L108-111.

**Query 5:**

*The authors should add the evidence-based descriptions that the early response (1-7 days post vaccination) of immune-related genes showed in the fig. 4 and 5 would be of benefit to DNA vaccination in the discussion part.*

Whereas some mention had been made to the benefit of these early responses, we agree that the original manuscript did not clarify the findings and evaluations of these in a satisfactory manner. The discussion has therefore to some extent been rewritten to clarify potential benefits *as well as* negative effects of the various early immune responses.

The role of proinflammatory cytokines in the migration of inflammatory cells to the site of injection has been specified in the description of biological function (L95-97), whereas the potential influence of these cytokines on DNA vaccines and transgene expression is described in L434-442. Likewise, the antiviral functions of IFN- $\alpha$  and Mx and the relation to CD8 and Eomes expression can be found in the introduction, as described for query 4. In the discussion, L448-449 and L451-453 reference the importance of innate antiviral responses in teleosts and presents the potential benefit to later, acquired

responses. In L455-457 a reference is given to the potential influence of PLGA particle size on the resulting antiviral response.

---

Reviewer #2: I consider that author's answers for my comments were sufficient, and revisions made the manuscript clearer.

The present study is now worthwhile publishing in Fish and shellfish immunology.

However, there are two comments for the revised manuscript as shown in below.

1. The authors used a term "vaccination" for pDNA delivery in the present study. Is this "vaccination" appropriate term for the experiment performed in the presents study?

Response: We have changes the term "DNA vaccination" to "genetic engineering"

2. For "Histopathology" in the section of results. The authors' classified histological changes post injection. However, there is a low objectivity in this analysis. Therefore, the authors should make the all calcification index clear by showing all images of histological classification, if possible.

I suppose that the result, "The histopathological changes caused by particles seemed to depend on particle size (nano vs. micro) rather than content (empty vs. pDNA)." is very important for the present study. Therefore, the authors should show detailed results for this analysis.

Response: A calcification index is a measure of accumulation of calcium salts in a body tissue and thus not very relevant for this study, we think. However in certain cases, a calcification process may occur during inflammation and would preferably be observed and diagnosed by X-ray analysis. We have addressed the histopathological score vs. different particle sizes (table 4), but it is difficult to give exact quantitative score, as histological examination is a qualitative method. We are sorry that we cannot meet this criticism by applying other quantitative measures.



24 **Abstract**

25 The use of poly-(D,L-lactic-*co*-glycolic) acid (PLGA) particles as carriers for DNA  
26 delivery has received considerable attention in mammalian studies. DNA vaccination of  
27 fish has been shown to elicit durable transgene expression, but no reports exist on  
28 intramuscular administration of PLGA-encapsulated plasmid DNA (pDNA). We injected  
29 Atlantic salmon (*Salmo salar* L.) intramuscularly with a plasmid vector containing a  
30 luciferase (*Photinus pyralis*) reporter gene as a) naked pDNA, b) encapsulated into  
31 PLGA nano- (~320nm) (NP) or microparticles (~4µm) (MP), c) in an oil-based  
32 formulation, or with empty particles of both sizes. The ability of the different pDNA-  
33 treatments to induce transgene expression was analyzed through a 70-day experimental  
34 period. Anatomical distribution patterns and depot effects were determined by tracking  
35 isotope labeled pDNA. Muscle, head kidney and spleen from all treatment groups were  
36 analyzed for proinflammatory cytokines (TNF $\alpha$ , IL-1 $\beta$ ), antiviral genes (IFN- $\alpha$ , Mx) and  
37 cytotoxic T-cell markers (CD8, Eomes) at mRNA transcription levels at days 1, 2, 4 and  
38 7. Histopathological examinations were performed on injection-site samples from days 2,  
39 7 and 30. Injection of either naked pDNA or the oil-formulation was superior to particle  
40 treatments for inducing transgene expression at early time-points. Empty particles of both  
41 sizes were able to induce proinflammatory immune responses as well as degenerative and  
42 inflammatory pathology at the injection site. Microparticles demonstrated injection-site  
43 depots and an inflammatory pathology comparable to the oil-based formulation. In  
44 comparison, the distribution of NP-encapsulated pDNA resembled that of naked pDNA,  
45 although encapsulation into NPs significantly elevated the expression of antiviral genes  
46 in all tissues. Together the results indicate that while naked pDNA is most efficient for



47 inducing transgene expression, the encapsulation of pDNA into NPs up-regulates  
48 antiviral responses that could be of benefit to DNA vaccination.

49

50

51

52

53

54

55

56

57

58

59

60

61

62

63

64

65

66

67

68

69

70 **Introduction**

71 PLGA (poly-(D,L-lactic-*co*-glycolic)-acid) nano- and microparticles as adjuvants and  
72 carriers for vaccine antigens have been extensively investigated, mainly in mammalian  
73 models [1-5]. The biodegradable copolymer produces non-toxic degradation products [3],  
74 offers increased predictability of antigen release-rates, potential for intracellular antigen  
75 delivery and the ability to encapsulate and co-encapsulate a wide variety of antigens,  
76 including DNA vaccines [1, 6, 7].

77 **Luciferase has commonly been applied for the evaluation of DNA vaccines at**  
78 **both transcription and protein level, and appears to express higher in fish than in**  
79 **mammals for a given dose of DNA** [8-12]. The encapsulation of plasmid DNA into  
80 PLGA particles could protect against the rapid on-site degradation reported in both mice  
81 and salmon after intramuscular injection, and has been shown to increase the escape of  
82 antigen from endosomes to the cytosol [6, 8, 10, 11, 13].

83 Depending on size, the particles may create injection-site depots (>5 $\mu$ m), get  
84 phagocytized by antigen presenting cells (APCs) (<5 $\mu$ m), be internalized by non-  
85 phagocytic cells such as myocytes (<500nm) or escape into the bloodstream and  
86 subsequently be cleared by phagocytes in the head kidney, spleen and/or liver [4, 14].  
87 Muscle cells have been shown to slowly accumulate pDNA over time, and could benefit  
88 from extracellular pDNA-releasing microparticles as well as intracellular nanoparticle  
89 depots [15].

90 A central attribute of DNA vaccines is the ability to induce cellular as well as  
91 humoral immune responses, including cytotoxic T-lymphocyte (CTL) responses and  
92 antibody production [16-18]. Unlike vertebrate DNA, bacterial DNA contains stretches of

93 unmethylated CpG sequences that are recognized as danger signals by toll-like receptor 9  
94 (TLR9). Upon stimulation this endosomal pattern recognition receptor (PRR) may induce  
95 a variety of cytokines. Interleukin-1 $\beta$  (IL-1 $\beta$ ) and tumor necrosis factor- $\alpha$  (TNF- $\alpha$ ) are  
96 hallmark cytokines in driving the inflammatory response in mammals and amongst other  
97 properties hold key roles in the migration of effector cells to sites of infection [19]. Both  
98 cytokines have been found in a number of teleost species and appear to exert functions  
99 similar to what is known from mammals [20-22].

100 Interferon- $\alpha$  (IFN- $\alpha$ ) is one of the type I IFNs, key mediators of antiviral  
101 responses through the regulation of IFN-stimulated genes and central in linking innate  
102 and adaptive immunity [16, 23-25]. The IFN-induced protein Mx has demonstrated  
103 antiviral functions in Atlantic salmon (*Salmo salar* L.) and can be used to follow IFN  
104 activity, as it has a much longer lifetime and accumulates to higher concentrations [26-  
105 28]. Type I IFNs also play an important role in the clonal expansion and generation of  
106 specific as well as non-specific memory CD8<sup>+</sup> T-cells [29]. Sequences for CD8 $\alpha$  and  
107 CD8 $\beta$  are known from a variety of teleost species and the cytotoxic activity of CD8<sup>+</sup> T-  
108 cells has been demonstrated in rainbow trout (*Oncorhynchus mykiss*) [30, 31]. The  
109 transcription factor Eomesodermin (Eomes) is critical to the development of CD8<sup>+</sup> T-cell  
110 effector functions and memory cells in mammals [32, 33]. A recent study indicated  
111 similar functions as well as induction by IFN- $\alpha$  in Atlantic salmon [34].

112 Intramuscular injection of naked pDNA generally induces few and transient  
113 histopathological changes in fish as well as in mammals [9]. In contrast, the use of PLG  
114 microspheres as DNA carriers has been shown to result in a foreign body response in  
115 mice, where the infiltrating cells were also the ones that were primarily transfected [35].

116 Enhanced inflammatory reactions coupled with prolonged availability of pDNA might  
117 therefore be beneficial to transgene expression and T-cell responses.

118 This report is the first on intramuscular injection of Atlantic salmon with PLGA  
119 nano- and microparticles carrying pDNA, and the effect of these particles on 1) tissue  
120 distribution and retention of pDNA 2) expression of a firefly (*Photinus pyralis*) luciferase  
121 reporter gene 3) innate inflammatory (TNF- $\alpha$ , IL-1 $\beta$ ) and antiviral (IFN- $\alpha$ , Mx) immune  
122 responses, 4) expression of cytotoxic T-cell markers (CD8, Eomes) and 5) injection site  
123 histopathology. We hypothesize that PLGA-encapsulated pDNA will induce transgene  
124 expression and proinflammatory as well as antiviral responses more efficiently than non-  
125 encapsulated pDNA.

126

127

## 128 **2. Experimental**

### 129 *2.1 Materials/Chemicals*

130 Poly(D,L-lactic-co-glycolic) acid (PLGA; 50:50 ratio,  $M_w$  of 7-17 kDa), poly vinyl  
131 alcohol (PVA, 87-89 % hydrolyzed), D-(+)-trehalose dehydrate, 1,3,4,6-tetrachloro-3 $\alpha$ ,  
132 6 $\alpha$ -diphenylglycouril (Iodogen; Pierce, Rockford, IL, USA), Freund's incomplete  
133 adjuvant (FIA) and quantitative polymerase chain-reaction (QPCR) primers were  
134 purchased from Sigma Aldrich. Carrier free Na[<sup>125</sup>I] was from Perkin-Elmer Norge  
135 (Oslo, Norway). Acetone, dichloromethane (DCM) and chloroform were purchased from  
136 Merck Biochemicals. Sodium metabisulphite (Na<sub>2</sub>S<sub>2</sub>O<sub>5</sub> > 98 % purity) and potassium  
137 iodide (KI > 99.5 % purity) were purchased from Fluka Biochemica. Luciferase  
138 lyophilizate was purchased from Roche Diagnostics GmbH (Mannheim, Germany).

139 2.2 *Plasmid DNA*

140 Plasmid R70pRomiLuc (gift from Uwe Fischer, Friedrich-Loeffler-Institut, Germany)  
141 contains a firefly luciferase gene under the control of a murine cytomegalovirus  
142 immediate early promoter (CMV-IEP). The plasmid was isolated from a culture of  
143 *Escherichia coli* (strain DH5 $\alpha$ ) by use of Qiagen Plasmid Giga Kit (Qiagen GmbH,  
144 Hilden, Germany) according to manufacturer instructions. Purified plasmid was eluted in  
145 Tris-EDTA (TE) buffer (pH=8.0). DNA concentration and quality was determined with a  
146 NanoDrop<sup>®</sup> ND-1000 spectrophotometer (NanoDrop Technologies, Wilmington, DE,  
147 USA) and 1% agarose gel-electrophoresis. High quality samples ( $A_{260}/A_{280}$  ratio > 1.9  
148 and distinct DNA bands on gel) were stored at -20 °C until use.

149

150 2.3 *Preparation of [<sup>125</sup>I]-fluorescein-pDNA*

151 Purified pDNA was modified using the nucleic acid labeling kit *LabelIT* Fluorescein  
152 (MIR 3200, Mirus Corp., Madison, WI, USA) according to manufacturer instructions.  
153 Radiolabeling of f-pDNA with carrier-free Na[<sup>125</sup>I] was performed in a direct reaction  
154 with 1,3,4,6-tetrachloro-3 $\alpha$ ,6 $\alpha$ -diphenylglycoluril as the oxidizing agent. The protocol  
155 was in accordance with the Iodogen method of radiolabeling [36], with minor  
156 modifications concerning incubation time (1h). Free iodine was removed by filtration on  
157 a PD-10 column equilibrated with pDNA in PBS. Radiation was determined by gamma  
158 counting (COBRA<sup>™</sup> II Auto-Gamma<sup>®</sup>, ©Packard Instrument Co., Meridan, IL, USA),  
159 with specific activity measured to ~ 4.75 million cpm  $\mu\text{g}^{-1}$  <sup>125</sup>I-f-pDNA.

160

161

162 *2.4 Preparation of naked and pDNA-loaded nano- and microparticles*

163 Particles were prepared by a modified version of the double emulsion ( $W_1/O/W_2$ ) solvent  
164 evaporation method [2, 5, 37], outlined in table 1. A fraction of  $^{125}\text{I}$ -f-pDNA was  
165 included in the first water phase ( $W_1$ ) for determination of encapsulation efficiency and  
166 tracing of tissue distribution in *in vivo* experiments. Emulsions were prepared on ice-  
167 baths by sonication (S) (Sonics VibraCell VC750, 3 mm tapered micro tip, Sonics &  
168 Materials Inc., Newtown, CT, USA) or homogenization (H) (Ultra-turrax® T-25 Basic,  
169 IKA®-WERKE, Staufen, Germany). Plasmid was excluded from the  $W_1$  phase for  
170 preparation of naked particles. Fifteen ml  $\text{dH}_2\text{O}$  was added to the  $W_1/O/W_2$ -emulsions  
171 before overnight stirring to facilitate solvent evaporation. After centrifugation (Avanti®  
172 J-26 XP, BeckmanCoulter®, USA), pellets were re-suspended in  $\text{dH}_2\text{O}$  and the fractions  
173 were pooled. Trehalose ( $5 \text{ mg ml}^{-1}$  in  $\text{dH}_2\text{O}$ ) was used as a lyoprotectant and added to  
174 suspension aliquots in a ratio of 1:3. Aliquots were kept at  $-80^\circ\text{C}$  for a minimum of 2 h  
175 before lyophilization for 72 h at 0.001 hPa,  $-110^\circ\text{C}$  (ScanVac CoolSafe™, LaboGene,  
176 Denmark). Lyophilizates were stored in airtight containers at  $4^\circ\text{C}$ .

177

178 *2.5 Particle characterization*

179 Encapsulation of pDNA was determined by the gamma emission in a known amount of  
180 particles (COBRA™ II Auto-Gamma®) and measured radioactivity related to the  
181 specific radioactivity in the fraction of  $^{125}\text{I}$ -f-pDNA stock solution added to the  $W_1$ -phase.  
182 Encapsulation efficiency was determined as entrapped amount of pDNA relative to the  
183 amount initially present in the  $W_1$ -phase. Loading ( $\mu\text{g pDNA mg}^{-1}$  PLGA) was calculated  
184 by relating encapsulated pDNA to the total weight of retrieved particles. Sizing of

185 nanoparticles was performed by photon correlation spectroscopy (PCS) (NiComp 380  
186 Submicron Particle Sizer, Santa Barbara, USA). Microparticle size was determined by  
187 use of a Model 780 AccuSizer (NiComp).

188

### 189 *2.6 In vitro particle stability and pDNA release*

190 Five containers of 10 mg lyophilizate dissolved in 1 ml PBS (pH 7.4) with 0.02% sodium  
191 azide (NaN<sub>3</sub>) were prepared for both nano- and microparticles. The suspensions were  
192 incubated at 8°C on a Stuart® SB3 rotator. Sampling was performed immediately after  
193 particles had been dissolved, and then at 3 h, day 1, 2, 4, 7, 14, 21, 30, 40, 50, 60 and 70.  
194 At each sampling 100 µl were removed and centrifuged at 15,000 x g for 1 minute. Fifty  
195 µl of the supernatant were removed for isotope measurement, and the remaining fraction  
196 transferred back to the original container after addition of 50 µl new PBS and full re-  
197 suspension of the particle pellets.

198

### 199 *2.7 Fish*

200 Unvaccinated pre-smolt Atlantic salmon with a mean weight of 30 g were provided by  
201 and kept at Tromsø Aquaculture Research Station. The fish were kept in 200 L plastic  
202 tanks supplied with running fresh water (8-10°C) and fed a commercial feed from  
203 Skretting AS (Stavanger, Norway). Adaptation to test conditions was performed for one  
204 week prior to immunization. All experiments were in compliance with The Norwegian  
205 Welfare of Animals Act.

206

207

208 2.8 *Experimental groups and genetic engineering (GE)*

209 A total of 336 fish were distributed among seven tanks. Each tank contained 6 fish from  
210 each of the eight experimental groups (Table 2). Prior to tattooing and GE the fish were  
211 sedated with benzocaine using 40 mg L<sup>-1</sup> (Benzoak Vet., ACD Pharmaceuticals, Leknes,  
212 Norway). The PanJet needle free injection system with saturated Alcian blue was used for  
213 tattooing. All formulations were administered in 50 µl volumes by injection in the left  
214 epaxial muscle. Each injection dose contained 11 µg pDNA, and the amount of NPs and  
215 MPs was adjusted to make up for differences in pDNA loading. Injection dose samples  
216 were collected from each formulation in order to determine cpm.

217

218 2.9 *Sampling*

219 The fish were starved for 24 h prior to sampling and killed by a double dose (80 mg L<sup>-1</sup>)  
220 of benzocaine. At day 1, 2, 4, 7, 14, 30 and 70 post injection one tank was sampled. All  
221 fish were weighed. Blood from fish given radioactive formulations was sampled using  
222 vacutainers (Becton Dickinson) and stored on ice. Two muscle samples from the  
223 injection site were transferred to 10% neutral buffered formalin for storage until  
224 histological processing. Muscle samples, spleens and head kidneys were transferred to  
225 separate tubes containing 1 ml RNAlater® (Ambion, Austin, TX, USA) and kept at room  
226 temperature overnight before storage at -20°C. To determine tissue distribution in fish  
227 given radioactive formulations it was necessary to sample the full carcass. Trunk kidney,  
228 organ package (liver, heart, gastrointestinal tract (GIT) and interstitial adipose tissue),  
229 head (incl. gills) and remaining muscle (with skin) were collected in separate tubes. One



230 fish injected only with PBS was similarly sampled at each time point in order to exclude  
231 the possibility of radioactive contamination by cohabitation.

232

### 233 *2.10 Anatomic distribution and plasmid DNA retention*

234 Determination of *in vivo* retention and biodistribution was achieved by tracking trace  
235 amounts of  $^{125}\text{I}$ -f-pDNA. From blood samples, 50  $\mu\text{l}$  were removed for analysis.  
236 Radioactivity in blood and trunk kidney samples was determined with a COBRA™ II  
237 gamma counter. Remaining samples, including spleen and injection site tissue, were  
238 analyzed using a Packard Auto-Gamma Scintillation Spectrometer (©Packard Instrument  
239 Co., model 5120). Background radiation was measured to be 50 and 100 cpm  
240 respectively for the two machines. These were set as baselines, and were subtracted from  
241 measured values before data were adjusted according to [ $^{125}\text{I}$ ] half-life. Blood volume  
242 was set to 4% of the body weight [38]. Mean values of the injection dose samples  
243 gathered during **GE** were used to determine total cpm recovery (%) at day 1. To  
244 determine the stability of retention, the daily cpm means were related to recovery at day  
245 1. Daily cpm means were used to determine anatomical distribution.

246

### 247 *2.11 RNA isolation and cDNA synthesis*

248 Tissue samples (20-30 mg) were removed from RNAlater® and homogenized in lysis  
249 buffer from the RNeasy mini kit (Qiagen) using tubes with ceramic beads (Precellys) and  
250 a Precellys® 24 Homogenizer (Bertin Technologies). Parameters were set for 5300 x g x  
251 3 spins, 10 s. Subsequent RNA extractions and on-column purification with the RNase-  
252 Free DNase Set from Qiagen were performed according to manufacturer instructions.

253 RNA was eluted in 50  $\mu$ l RNase-free water and stored at  $-80^{\circ}\text{C}$  until use. RNA  
254 concentration and quality was determined using NanoDrop® (NanoDrop Technologies)  
255 and 1% agarose gel electrophoresis. High quality samples (260/280 ratio  $> 1.9$  and tight  
256 18S/28S bands) were used for cDNA synthesis. Reverse transcription was performed  
257 with the High Capacity RNA-to-cDNA Master-mix from Applied Biosystems in  
258 accordance with manufacturer instructions. Each reaction contained 400 ng RNA in 20  
259  $\mu$ l. Samples were diluted to 80  $\mu$ l with RNase-free water and stored at  $-80^{\circ}\text{C}$ .

260

### 261 *2.12 Quantitative reverse transcription polymerase chain reaction (QPCR)*

262 Quantitative PCR was performed according to manufacturer instructions using Fast  
263 SYBR® Green Master Mix (Applied Biosystems) and primers previously applied in our  
264 laboratory (Table 3). Primer efficiency was determined using a six-point 1:2 dilution  
265 series in triplicate, with an initial cDNA concentration of 20 ng. All primers were free of  
266 primer-dimers in no-template control and showed a single peak in the dissociation curve.  
267 Samples containing 20 ng cDNA were run in triplicate, with each plate including no-  
268 template control and an inter-run calibrator. Analysis was performed on a 7500 Fast Real-  
269 Time PCR System (Applied Biosystems) with the thermal cycler profile set to  $95^{\circ}\text{C}$  for  
270 20 s, 40 cycles of  $95^{\circ}\text{C}$  for 3 s and 40 cycles of  $60^{\circ}\text{C}$  for 30 s. Dissociation curves were  
271 performed on all samples. The 7500 Software Relative Quantification Study Application  
272 (v2.0.4, Applied Biosystems) was used to determine  $C_T$  values, with walking baseline  
273 and threshold set manually to be equal for all genes. Relative gene expression was  
274 determined by the Pfaffl method [39], comparing saline injected fish to treated groups.  
275 To determine relative expression of luciferase the highest day 1 transcript average was

276 used as control. Head kidney and spleen samples from day 2 and 7 were also checked for  
277 luciferase transcripts.

278

### 279 *2.13 Histology*

280 Muscle samples from days 2, 7 and 30 post injection were chosen for histology. The  
281 service of routine histological processing and staining with hematoxylin and eosin (HE)  
282 was purchased from the National Veterinary Institute (Oslo, Norway). Sections were  
283 studied by light microscopy for signs of hemorrhages, tissue degradation and  
284 inflammation. Using the changes in day 2 saline injected fish as a baseline, observed  
285 changes were classified as either moderate (+) or strong (++). Moderate changes were  
286 determined as largely limited to the needle trajectory, with inflammatory cells primarily  
287 associated with degenerated tissue and/or dispersed among intact muscle cells. Strong  
288 changes were seen as degeneration and/or inflammation spreading beyond the needle  
289 trajectory, with few or no intact muscle cells present within the cellular infiltrate. The  
290 histopathology scores were performed as blind testing by two professionals.

291

### 292 *2.14 Statistical analysis*

293 Microsoft Excel (Microsoft™) was used for arrangement of data as well as calculation of  
294 biodistribution and relative gene expression. Statistical analyses for real-time PCR were  
295 performed with IBM SPSS (Statistical Package for the Social Sciences, version 19.0). All  
296 data were natural log transformed prior to analysis, and normality verified by the  
297 Shapiro-Wilk test. Levene's test of equality of variances was used to check for  
298 homoscedasticity. Homoscedastic data were analyzed by one-way ANOVA with Tukey

299 as the post hoc test. Where homoscedasticity was violated, the Welch test of equality of  
300 means was applied, followed by Dunnett T3 post hoc. Graphs were constructed with  
301 Microsoft Excel and SPSS.

302

303

### 304 **3. Results**

#### 305 *3.1 Particle characterization*

306 The encapsulation efficiency and loading of <sup>125</sup>I-f-pDNA were low for both particles  
307 sizes. The different particle characteristics are summarized in table 1, where empty  
308 particles have been excluded due to minor size differences. The mean size of  
309 nanoparticles was 320 nm by intensity distribution, with more than 90% measuring less  
310 than 500 nm. The number weight mean diameter of microparticles was 3-4 μm, with 80%  
311 measuring less than 5 μm and more than 90% smaller than 10 μm.

312

#### 313 *3.2 In vitro particle stability and pDNA release*

314 Neutral pH and a temperature of 8°C were chosen in order to simulate *in vivo* conditions.  
315 Initial burst release was 81% for NP-(<sup>125</sup>I-f-pDNA) and 49% for MP-(<sup>125</sup>I-f-pDNA). Both  
316 groups subsequently displayed a slow and sustained release, with a 96% and 69 %  
317 accumulated release at day 70 (Fig. 1).

318

#### 319 *3.3 Anatomical distribution and depot of vaccine formulations*

320 No radioactivity was registered in blood later than day 7-post injection. The average total  
321 cpm recovery at day 1 ranged from 15% for NP-(<sup>125</sup>I-f-pDNA) to 39% for <sup>125</sup>I-f-pDNA

322 (results not shown). Radioactivity was primarily recovered from the injection site, organs  
323 and trunk kidney. High degrees of similarities in tissue distribution were observed for  
324 NP-(<sup>125</sup>I-f-pDNA) and <sup>125</sup>I-f-pDNA (Fig. 2A, B). Likewise, MP-(<sup>125</sup>I-f-pDNA) and FIA-  
325 (<sup>125</sup>I-f-pDNA) had similar distribution profiles and injection site depots (Fig. 2C, D). The  
326 trunk kidney was the primary site of recovery for NP-(<sup>125</sup>I-f-pDNA) and <sup>125</sup>I-f-pDNA,  
327 containing almost 80% of total radiation at day 70. NP-(<sup>125</sup>I-f-pDNA) showed higher  
328 injection site retention (5%) at day 70 compared to <sup>125</sup>I-f-pDNA (1%). The respective  
329 values for MP-(<sup>125</sup>I-f-pDNA) and FIA-(<sup>125</sup>I-f-pDNA) were 34% and 26%, with retention  
330 in trunk kidney reaching 32% and 27% at day 70.

331

### 332 *3.4 Quantitative reverse transcription polymerase chain reaction (QPCR)*

#### 333 *3.4.1 Expression of luciferase reporter gene*

334 FIA-(<sup>125</sup>I-f-pDNA) induced the highest luciferase transcript average in muscle at day 1  
335 and was chosen as calibrator for this tissue. FIA-(<sup>125</sup>I-f-pDNA) also induced the highest  
336 individual levels of luciferase transcripts throughout the experiment, with significant  
337 expression at day 1, 4 and 14 ( $p \leq 0.032$ ) (Fig. 3). Naked plasmids consistently induced  
338 higher expression than the particle formulations, with significance for pDNA at day 1-7  
339 ( $p \leq 0.042$ ) and <sup>125</sup>I-f-pDNA at day 4 ( $p = 0.018$ ). No significant differences were found  
340 at days 30 and 70. Low luciferase transcript levels were detected in head kidney, with  
341 pDNA and <sup>125</sup>I-f-pDNA inducing significant expression compared to NP-<sup>125</sup>I-f-pDNA at  
342 day 2 ( $p \leq 0.016$ , results not shown). No expression was detected in the spleen.

343

344

345 *3.4.2 Proinflammatory cytokines IL-1 $\beta$  and TNF- $\alpha$*

346 The particle formulations significantly up-regulated IL-1 $\beta$  in muscle samples at all time-  
347 points; NP-(<sup>125</sup>I-f-pDNA) ( $p \leq 0.002$ ), NP ( $p \leq 0.004$ ), MP-(<sup>125</sup>I-f-pDNA) ( $p \leq 0.003$ ),  
348 MP ( $p \leq 0.015$ ) (Fig. 4A). From day 2 the up-regulation was significant compared to all  
349 non-particle groups. MP formulations consistently induced the highest expression. FIA-  
350 (<sup>125</sup>I-f-pDNA) significantly up-regulated IL-1 $\beta$  in muscle at day 7 ( $p = 0.000$ ). Significant  
351 expression of TNF- $\alpha$  in head kidney was only found at day 4, with NP-(<sup>125</sup>I-f-pDNA) ( $p$   
352 = 0.034) and MP ( $p = 0.008$ ) (Fig. 4B). No significant expression of TNF- $\alpha$  was found in  
353 the spleen or muscle.

354

355 *3.4.3 IFN- $\alpha$  and Mx*

356 NP-(<sup>125</sup>I-f-pDNA) significantly up-regulated IFN- $\alpha$  at the injection site at day 4 ( $p =$   
357 0.005). Levels in head kidney were generally low, with significant up-regulation by <sup>125</sup>I-  
358 f-pDNA ( $p = 0.000$ ) at day 2. NP-(<sup>125</sup>I-f-pDNA) ( $p \leq 0.003$ ) and NP ( $p \leq 0.036$ )  
359 significantly up-regulated IFN- $\alpha$  in spleen at day 1 and 2 (results not shown). Levels of  
360 Mx at the injection site increased for all groups from day 1 to 7. NP-(<sup>125</sup>I-f-pDNA)  
361 induced significant expression at day 2-7 ( $p = 0.000$ ), and was superior to all groups at  
362 day 4 and 7 ( $p \leq 0.020$ ). MP-(<sup>125</sup>I-f-pDNA) significantly up-regulated Mx in muscle at  
363 day 2 and 4 ( $p \leq 0.006$ ) (Fig. 5A). NP-(<sup>125</sup>I-f-pDNA) appeared the most potent treatment  
364 for inducing Mx in head kidney, but no significance was found (Fig. 5B). Mx expression  
365 increased in spleen for all groups from day 1 to 7, with significance for NP-(<sup>125</sup>I-f-pDNA)  
366 at day 4 ( $p = 0.013$ ) (Fig. 5C).

367

368 *3.4.4 CD8 and Eomes*

369 There was no significant up-regulation of CD8 in any tissue. Several muscle samples  
370 showed no CD8 expression, and no statistical analyses could therefore be performed.

371 No expression of CD8 could be detected at day 2 in head kidney samples from fish  
372 injected with <sup>125</sup>I-f-pDNA. Interestingly, these samples induced the only significant up-  
373 regulation of Eomes observed within any tissue (p = 0.000) (results not shown).

374

375 *3.6 Histopathology*

376 Tissue sections of injection site samples were examined by light microscopy for signs of  
377 hemorrhages, muscle degeneration and inflammation (Table 4). PBS caused only minor  
378 hemorrhages and tissue degeneration at day 2 (Fig. 6A), indicating that later changes  
379 were likely the results of the different treatments. Hemorrhages were most pronounced at  
380 day 2 in all groups. Administration of PBS and <sup>125</sup>I-f-pDNA caused moderate muscle  
381 degeneration, but no inflammation. Both tissue degeneration and inflammation were  
382 observed for pDNA (Fig. 6C), but both pathologies were more frequent with particles  
383 formulations. MP-(<sup>125</sup>I-f-pDNA) and FIA-(<sup>125</sup>I-f-pDNA) both demonstrated strong  
384 inflammation at day 30 (Fig. 6B, D), with a high influx of inflammatory cells that for  
385 FIA-(<sup>125</sup>I-f-pDNA) was concentrated around possible oil-droplets. The histopathological  
386 changes caused by particles seemed to depend on particle size (nano vs. micro) rather  
387 than content (empty vs. pDNA).

388

389

390

391 **4. Discussion**

392 The use of PLGA particle constructs as carriers for DNA vaccine delivery has so far  
393 received little attention in fish studies [1, 40]. We have investigated distribution/depot,  
394 transgene and immune gene transcription as well as injection site histopathology  
395 following intramuscular injection of Atlantic salmon with PLGA particles carrying  
396 pDNA-encoding luciferase. The double emulsion solvent evaporation method [2, 37] was  
397 used to prepare nano- and microparticles with mean diameters of 320 nm and 4  $\mu$ m,  
398 respectively. Low pDNA encapsulation appears to be a recurring problem, and our results  
399 (<30% for both particle sizes) are supported by other studies [12, 35].

400 One of the challenges of conventional DNA vaccination is the rapid tissue  
401 clearance and on-site degradation of DNA, which may result in reduced pDNA uptake  
402 and transgene expression [8, 10]. **Although oil adjuvants are not commonly applied for**  
403 **intramuscular vaccine delivery, FIA-(<sup>125</sup>I-f-pDNA) provided a positive control to**  
404 **measure the depot potential of nano- and microparticles.** The high burst release observed  
405 for NP-(<sup>125</sup>I-f-pDNA) during the *in vitro* release study (Fig. 1) likely explains the strong  
406 similarities between this group and <sup>125</sup>I-f-pDNA (Fig. 2A, B), a similarity reflected also  
407 in the injection site histopathology (Table 4). In comparison, the injection site retention  
408 of MP-(<sup>125</sup>I-f-pDNA) remained similar to that of FIA-(<sup>125</sup>I-f-pDNA) throughout the study  
409 (Fig. 2C, D). The duration of the MP-(<sup>125</sup>I-f-pDNA) and FIA-(<sup>125</sup>I-f-pDNA) depots likely  
410 contributed to the severe histopathological inflammations observed in tissue sections  
411 from both groups at day 30 (Fig. 6B, D). **Inflammatory cell infiltration has been shown to**  
412 **take place in both fish and mammals [35, 37, 41], and transient inflammatory responses**  
413 **may thus contribute to increased transgene expression. Long lasting inflammations such**



414 as seen with MP-(<sup>125</sup>I-f-pDNA) and FIA-(<sup>125</sup>I-f-pDNA) are, however, undesirable in a  
415 product meant for consumption. It would appear that nanoparticles may be favorable in  
416 order to avoid potential tissue damage, but the small sample sizes meant we could only  
417 obtain an indication of the histopathological influence of the various treatments.

418 Although the similarities in injection site retention were not reflected in the  
419 expression of the luciferase transgene (Fig. 3), the observation that FIA-(<sup>125</sup>I-f-pDNA)  
420 induced the highest individual levels of luciferase transcripts suggests that increased  
421 cellular infiltration along with a high injection site pDNA depot may be of benefit to  
422 transgene expression in Atlantic salmon. The significantly lower expression obtained  
423 with encapsulated pDNA could be a result of the preparation conditions, as the W<sub>1</sub>/O/W<sub>2</sub>  
424 method has been shown to cause a partial reduction in the content of supercoiled (SC)  
425 DNA topofrom that contributes to a lower transfection efficiency [1, 8, 37, 42]. The  
426 process of emulsification required lower shear forces and shorter duration of preparation  
427 and may thus have preserved a larger portion of SC DNA in FIA-(<sup>125</sup>I-f-pDNA). We did  
428 not, however, address whether the encapsulation of <sup>125</sup>I-f-pDNA resulted in an altered SC  
429 content. The absence of significant differences in luciferase expression at day 30 and 70  
430 still indicated a certain level of stability in particle groups that could result from a  
431 continued release of bioactive pDNA even at later time-points.

432 Another explanation for the low transcription levels obtained with encapsulated  
433 pDNA-Luc may lie with the inflammatory cytokine responses. Induced not only by  
434 stimulation of PRRs but also by PLGA itself [43, 44], IL-1 $\beta$  and TNF- $\alpha$  have both  
435 demonstrated inhibitory effects on transgene expression even at low concentrations,  
436 contributing to a reduced transfection efficiency of encapsulated DNA *in vivo* as opposed

437 to *in vitro* [2, 37, 45]. The nano- and microparticle formulations significantly up-  
438 regulated IL-1 $\beta$  at the injection site at all time-points (Fig. 4A), and while the expression  
439 of TNF- $\alpha$  was generally low a synergistic effect of different cytokines on the inhibition of  
440 transgene expression has been reported [45]. **In comparison, the levels of IL-1 $\beta$  in fish**  
441 **injected with FIA-(<sup>125</sup>I-f-pDNA) were not found significant until 7 days post**  
442 **administration, indicating that PLGA may provide a more potent inflammatory stimulus**  
443 **than the oil adjuvant even in the absence of pronounced inflammatory histopathology.**

444 **Viral challenge studies in fish have shown that specific protection may be**  
445 **acquired even with very low doses of DNA, and innate antiviral responses also appear to**  
446 **play a more critical role in fish than mammals upon exposure to viruses [46, 47].**  
447 Whereas luciferase is unlikely to induce a differentiation of antigen specific CD8<sup>+</sup> T-cells  
448 due to low immunogenicity in *in vivo* studies [48, 49], type I IFNs play an important role  
449 in the clonal expansion of CD8<sup>+</sup> T-cells and may enhance CTL responses when  
450 immunogenic transgene products are expressed [29]. Whereas the expression of IFN- $\alpha$   
451 was generally low and transient, NP-(<sup>125</sup>I-f-pDNA) still appeared the most potent inducer  
452 of antiviral responses and significantly up-regulated the expression of Mx in all tissues  
453 (Fig. 5). This result supports a previous study on the influence of particle size on the  
454 cytokine profile induced after administration of particle associated CpG DNA [50]. We  
455 did observe that formulations with naked pDNA significantly up-regulated both Eomes  
456 and IFN- $\alpha$  in head kidney at day 2, but no statistical correlation between these genes was  
457 found for any other group, tissue or time-point.

458 This study is the first on intramuscular injection of Atlantic salmon with PLGA  
459 particles carrying pDNA. Our particle formulations did not induce transgene expression

460 as efficiently as injection of naked plasmids, but appeared to provide a continued release  
461 of bioactive pDNA even at the end of the study. A strong expression of transgene may  
462 not always be necessary in order to mount a significantly protective immune response,  
463 and an efficient up-regulation of innate antiviral responses in particular might enhance  
464 the immunogenicity of an antiviral vaccine. Both particle sizes proved superior to naked  
465 pDNA injection for the induction of IL-1 $\beta$  as well as an influx of inflammatory cells at  
466 the injection site, but only encapsulation into nanoparticles significantly increased the  
467 expression of IFN- $\alpha$  and Mx. Together these results indicate that PLGA nanoparticles as  
468 carriers for plasmid vectors encoding viral antigens might enhance the responses to DNA  
469 vaccines.

470

471

## 472 **Acknowledgements**

473 This project was funded by the Research Council of Norway (project nos. 182035 and  
474 183204/S40) and Tromsø Research Foundation (“Induction and assessment of T cell  
475 immunity to virus antigens in salmonids). The authors would also like to acknowledge  
476 Merete Skar for technical help during particle sizing and Bjarte Lund for his assistance  
477 with RNA isolation.

478

479

480

- 481 1. Tian J, Yu J. Poly(lactic-co-glycolic acid) nanoparticles as candidate DNA  
482 vaccine carrier for oral immunization of Japanese flounder (*Paralichthys*  
483 *olivaceus*) against lymphocystis disease virus. *Fish Shellfish Immunol*  
484 2011;30:109-17.

- 485 2. Cohen H, Levy RJ, Gao J, Fishbein I, Kousaev V, Sosnowski S, et al. Sustained  
486 delivery and expression of DNA encapsulated in polymeric nanoparticles. *Gene*  
487 *Ther* 2000;7:1896-905.
- 488 3. Semete B, Booysen L, Lemmer Y, Kalombo L, Katata L, Verschoor J, et al. *In*  
489 *vivo* evaluation of the biodistribution and safety of PLGA nanoparticles as drug  
490 delivery systems. *Nanomed Nanotechnol* 2010;6:662-71.
- 491 4. Newman KD, Elamanchili P, Kwon GS, Samuel J. Uptake of poly(D,L-lactic-co-  
492 glycolic acid) microspheres by antigen-presenting cells *in vivo*. *J Biomed Mater*  
493 *Res* 2002;60:480-6.
- 494 5. Fredriksen BN, Sævareid K, McAuley L, Lane ME, Bøgwald J, Dalmo RA. Early  
495 immune responses in Atlantic salmon (*Salmo salar* L.) after immunization with  
496 PLGA nanoparticles loaded with a model antigen and  $\beta$ -glucan. *Vaccine*  
497 2011;29:8338-49.
- 498 6. Panyam J, Zhou WZ, Prabha S, Sahoo SK, Labhasetwar V. Rapid endo-lysosomal  
499 escape of poly(DL-lactide-co-glycolide) nanoparticles: implications for drug and  
500 gene delivery. *FASEB J* 2002;16:1217-26.
- 501 7. Schlosser E, Mueller M, Fischer S, Basta S, Busch DH, Gander B, et al. TLR  
502 ligands and antigen need to be coencapsulated into the same biodegradable  
503 microsphere for the generation of potent cytotoxic T lymphocyte responses.  
504 *Vaccine* 2008;26:1626-37.
- 505 8. Manthorpe M, Cornefertjensen F, Hartikka J, Felgner J, Rundell A, Margalith M,  
506 et al. Gene-therapy by intramuscular injection of plasmid DNA - studies on firefly  
507 luciferase gene-expression in mice. *Hum Gene Ther* 1993;4:419-31.
- 508 9. Garver K, Conway C, Elliott D, Kurath G. Analysis of DNA-vaccinated fish  
509 reveals viral antigen in muscle, kidney and thymus, and transient histopathologic  
510 changes. *J Mar Biotechnol* 2005;7:540-53.
- 511 10. Tonheim TC, Dalmo RA, Bøgwald J, Seternes T. Specific uptake of plasmid  
512 DNA without reporter gene expression in Atlantic salmon (*Salmo salar* L.) kidney  
513 after intramuscular administration. *Fish Shellfish Immunol* 2008;24:90-101.
- 514 11. Prabha S, Labhasetwar V. Critical determinants in PLGA/PLA nanoparticle-  
515 mediated gene expression. *Pharm Res* 2004;21:354-64.
- 516 12. Diez S, Tros de Ilarduya C. Versatility of biodegradable poly(D,L-lactic-co-  
517 glycolic acid) microspheres for plasmid DNA delivery. *Eur J Pharm Biopharm*  
518 2006;63:188-97.
- 519 13. Shen H, Ackerman AL, Cody V, Giodini A, Hinson ER, Cresswell P, et al.  
520 Enhanced and prolonged cross-presentation following endosomal escape of  
521 exogenous antigens encapsulated in biodegradable nanoparticles. *Immunology*  
522 2006;117:78-88.
- 523 14. Rejman J, Oberle V, Zuhorn IS, Hoekstra D. Size-dependent internalization of  
524 particles via the pathways of clathrin- and caveolae-mediated endocytosis.  
525 *Biochem J* 2004;377:159-69.
- 526 15. Satkauskas S, Bureau MF, Mahfoudi A, Mir LM. Slow accumulation of plasmid  
527 in muscle cells: Supporting evidence for a mechanism of DNA uptake by  
528 receptor-mediated endocytosis. *Mol Ther* 2001;4:317-23.

- 529 16. Krieg AM, Yi A-K, Matson S, Waldschmidt TJ, Bishop GA, Teasdale R, et al.  
530 CpG motifs in bacterial DNA trigger direct B-cell activation. *Nature*  
531 1995;374:546-9.
- 532 17. Utke K, Kock H, Schuetze H, Bergmann SM, Lorenzen N, Einer-Jensen K, et al.  
533 Cell-mediated immune responses in rainbow trout after DNA immunization  
534 against the viral hemorrhagic septicemia virus. *Dev Comp Immunol* 2008;32:239-  
535 52.
- 536 18. Klinman DM, Yamshchikov G, Ishigatsubo Y. Contribution of CpG motifs to the  
537 immunogenicity of DNA vaccines. *J Immunol* 1997;158:3635-9.
- 538 19. Shimizu Y, Newman W, Tanaka Y, Shaw S. Lymphocyte interactions with  
539 endothelial cells. *Immunol Today* 1992;13:106-12.
- 540 20. Mathew JA, Guo YX, Goh KP, Chan J, Verburg-van Kemenade BML, Kwang J.  
541 Characterisation of a monoclonal antibody to carp IL-1 $\beta$  and the development of a  
542 sensitive capture ELISA. *Fish Shellfish Immunol* 2002;13:85-95.
- 543 21. Zou J, Peddie S, Scapigliati G, Zhang Y, Bols NC, Ellis AE, et al. Functional  
544 characterisation of the recombinant tumor necrosis factors in rainbow trout,  
545 *Oncorhynchus mykiss*. *Dev Comp Immunol* 2003;27:813-22.
- 546 22. Zhang A, Chen D, Wei H, Du L, Zhao T, Wang X, et al. Functional  
547 characterization of TNF- $\alpha$  in grass carp head kidney leukocytes: Induction and  
548 involvement in the regulation of NF- $\kappa$ B signaling. *Fish Shellfish Immunol*  
549 2012;33:1123-32.
- 550 23. Latz E, Schoenemeyer A, Visintin A, Fitzgerald KA, Monks BG, Knetter CF, et  
551 al. TLR9 signals after translocating from the ER to CpG DNA in the lysosome.  
552 *Nat Immunol* 2004;5:190-8.
- 553 24. Hemmi H, Takeuchi O, Kawai T, Kaisho T, Sato S, Sanjo H, et al. A Toll-like  
554 receptor recognizes bacterial DNA. *Nature* 2000;408:740-5.
- 555 25. Whyte SK. The innate immune response of finfish – A review of current  
556 knowledge. *Fish Shellfish Immunol* 2007;23:1127-51.
- 557 26. Nygaard R, Husgard S, Sommer A-I, Leong J-AC, Robertsen B. Induction of Mx  
558 protein by interferon and double-stranded RNA in salmonid cells. *Fish Shellfish*  
559 *Immunol* 2000;10:435-50.
- 560 27. Larsen R, Rokenes TP, Robertsen B. Inhibition of infectious pancreatic necrosis  
561 virus replication by Atlantic salmon Mx1 protein. *J Virol* 2004;78:7938-44.
- 562 28. Horisberger MA, De Staritzky K. Expression and stability of the Mx protein in  
563 different tissues of mice, in response to interferon inducers or to influenza virus  
564 infection. *J Interferon Res* 1989;9:583-90.
- 565 29. Marshall HD, Prince AL, Berg LJ, Welsh RM. IFN- $\alpha\beta$  and self-MHC divert CD8  
566 T cells into a distinct differentiation pathway characterized by rapid acquisition of  
567 effector functions. *J Immunol* 2010;185:1419-28.
- 568 30. Moore LJ, Somamoto T, Lie KK, Dijkstra JM, Hordvik I. Characterisation of  
569 salmon and trout CD8 $\alpha$  and CD8 $\beta$ . *Mol Immunol* 2005;42:1225-34.
- 570 31. Takizawa F, Dijkstra JM, Kotterba P, Korytář T, Kock H, Köllner B, et al. The  
571 expression of CD8 $\alpha$  discriminates distinct T cell subsets in teleost fish. *Dev Comp*  
572 *Immunol* 2011;35:752-63.

- 573 32. Intlekofer AM, Takemoto N, Wherry EJ, Longworth SA, Northrup JT, Palanivel  
574 VR, et al. Effector and memory CD8<sup>+</sup> T cell fate coupled by T-bet and  
575 Eomesodermin. *Nat Immunol* 2005;6:1236-44.
- 576 33. Pearce EL, Mullen AC, Martins GA, Krawczyk CM, Hutchins AS, Zediak VP, et  
577 al. Control of effector CD8<sup>+</sup> T cell function by the transcription factor  
578 Eomesodermin. *Science* 2003;302:1041-3.
- 579 34. Kumari J, Bogwald J, Dalmo RA. Eomesodermin of Atlantic salmon: An  
580 important regulator of cytolytic gene and interferon gamma expression in spleen  
581 lymphocytes. *PLoS One* 2013;8:e55893.
- 582 35. Jang JH, Shea LD. Intramuscular delivery of DNA releasing microspheres:  
583 Microsphere properties and transgene expression. *J Control Release*  
584 2006;112:120-8.
- 585 36. Piatyszek MA, Jarmolowski A, Augustyniak J. Iodo-Gen-mediated  
586 radioiodination of nucleic acids. *Anal Biochem* 1988;172:356-9.
- 587 37. Labhasetwar V, Bonadio J, Goldstein SA, Levy JR. Gene transfection using  
588 biodegradable nanospheres: results in tissue culture and a rat osteotomy model.  
589 *Colloids Surf, B* 1999;16:281-90.
- 590 38. Ferguson H. Systemic pathology of fish: a text and atlas of comparative tissue  
591 responses in disease of teleosts. 1st ed: Ames: Iowa State University Press; 1989.
- 592 39. Pfaffl MW. A new mathematical model for relative quantification in real-time  
593 RT-PCR. *Nucleic Acids Res* 2001;29:e45.
- 594 40. Adomako M, St-Hilaire S, Zheng Y, Eley J, Marcum RD, Sealey W, et al. Oral  
595 DNA vaccination of rainbow trout, *Oncorhynchus mykiss* (Walbaum), against  
596 infectious haematopoietic necrosis virus using PLGA [Poly(D,L-Lactic-Co-  
597 Glycolic Acid)] nanoparticles. *J Fish Dis* 2012;35:203-14.
- 598 41. Boudinot P, Blanco M, de Kinkelin P, Benmansour A. Combined DNA  
599 immunization with the glycoprotein gene of viral hemorrhagic septicemia virus  
600 and infectious hematopoietic necrosis virus induces double-specific protective  
601 immunity and nonspecific response in rainbow trout. *Virology* 1998;249:297-306.
- 602 42. Weintraub H, Cheng PF, Conrad K. Expression of transfected DNA depends on  
603 DNA topology. *Cell* 1986;46:115-22.
- 604 43. Ding T, Sun J, Zhang P. Immune evaluation of biomaterials in TNF- $\alpha$  and IL-1 $\beta$   
605 at mRNA level. *J Mater Sci Mater Med* 2007;18:2233-6.
- 606 44. Sharp FA, Ruane D, Claass B, Creagh E, Harris J, Malyala P, et al. Uptake of  
607 particulate vaccine adjuvants by dendritic cells activates the NALP3  
608 inflammasome. *PNAS* 2009;106:870-5.
- 609 45. Tan Y, Li S, Pitt BR, Huang L. The inhibitory role of CpG immunostimulatory  
610 motifs in cationic lipid vector-mediated transgene expression *in vivo*. *Hum Gene*  
611 *Ther* 1999;10:2153-61.
- 612 46. McLauchlan PE, Collet B, Ingerslev E, Secombes CJ, Lorenzen N, Ellis AE.  
613 DNA vaccination against viral haemorrhagic septicaemia (VHS) in rainbow trout:  
614 size, dose, route of injection and duration of protection—early protection  
615 correlates with Mx expression. *Fish Shellfish Immunol* 2003;15:39-50.
- 616 47. Garver KA, LaPatra SE, Kurath G. Efficacy of an infectious hematopoietic  
617 necrosis (IHN) virus DNA vaccine in Chinook *Oncorhynchus tshawytscha* and  
618 sockeye *O. nerka* salmon. *Dis Aquat Org* 2005;64:13-22.

- 619 48. Wolff J, Malone R, Williams P, Chong W, Acsadi G, Jani A, et al. Direct gene  
620 transfer into mouse muscle *in vivo*. *Science* 1990;247:1465-8.
- 621 49. Heppell J, Lorenzen N, Armstrong NK, Wu T, Lorenzen E, Einer-Jensen K, et al.  
622 Development of DNA vaccines for fish: vector design, intramuscular injection  
623 and antigen expression using viral haemorrhagic septicaemia virus genes as  
624 model. *Fish Shellfish Immunol* 1998;8:271-86.
- 625 50. Chen HC, Sun B, Tran KK, Shen H. Effects of particle size on toll-like receptor  
626 9-mediated cytokine profiles. *Biomaterials* 2011;32:1731-7.
- 627
- 628

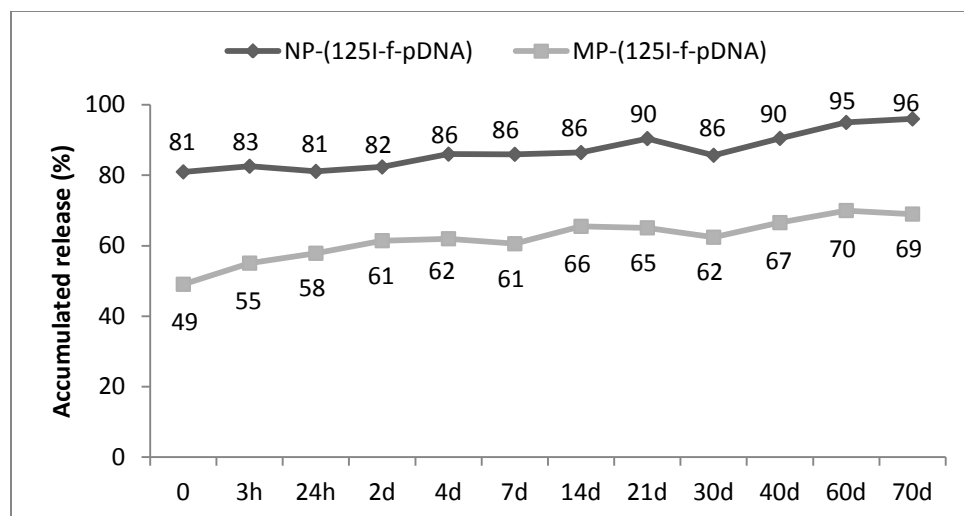


Figure 1 - Release of <sup>125</sup>I-f-pDNA from nano- and microparticles through 70 days of incubation at 8° C, presented as the mean accumulated release (%) of five samples at each time-point.



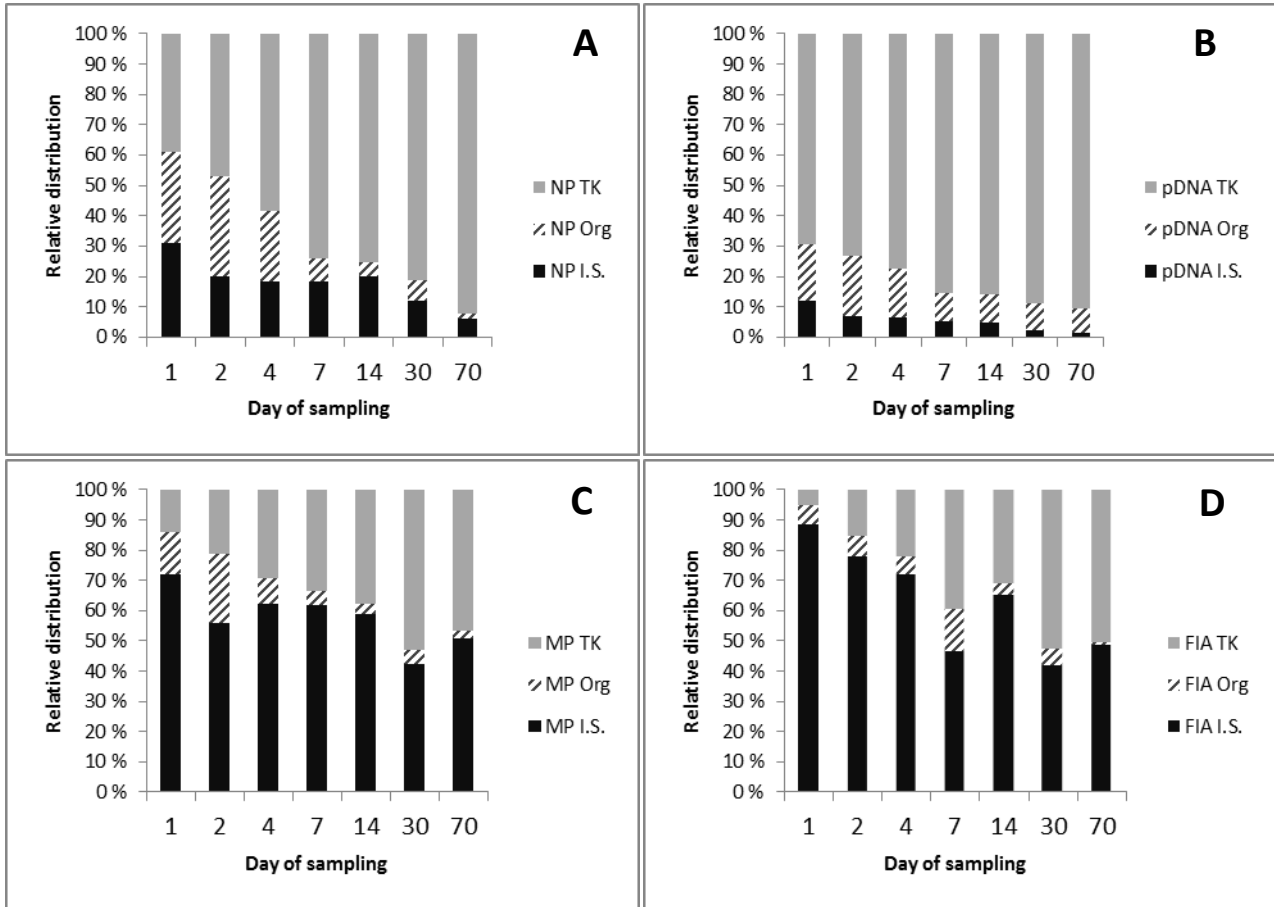


Figure 2 – Radioactivity recovered from samples of trunk kidney (TK), organs (Org) and injection site (I.S.). The stacked bars represent the relative distribution of pDNA among these organs in groups A) NP-(<sup>125</sup>I-f-pDNA), B) <sup>125</sup>I-f-pDNA, C) MP-(<sup>125</sup>I-f-pDNA) and D) FIA-(<sup>125</sup>I-f-pDNA). Five fish were sampled at each time-point.

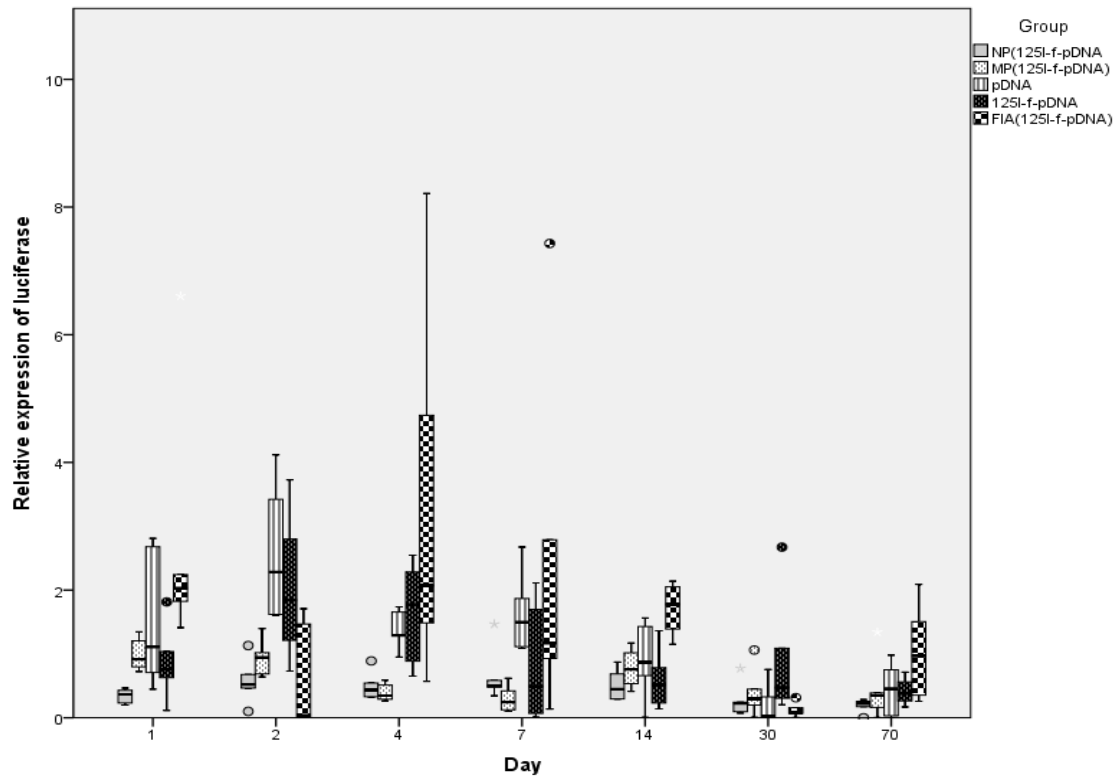


Figure 3 - Relative expression of luciferase mRNA transcripts in muscle from the injection site through the 70 day sample period. The box-plot shows the median value (line) and maximum and minimum values (whiskers), with the box representing 50% of the samples. Circles show outliers. The highest cpm-average at day 1 was found in group FIA-(<sup>125</sup>I-f-pDNA) and was set as calibrator. Six fish were sampled and analyzed at each time-point.

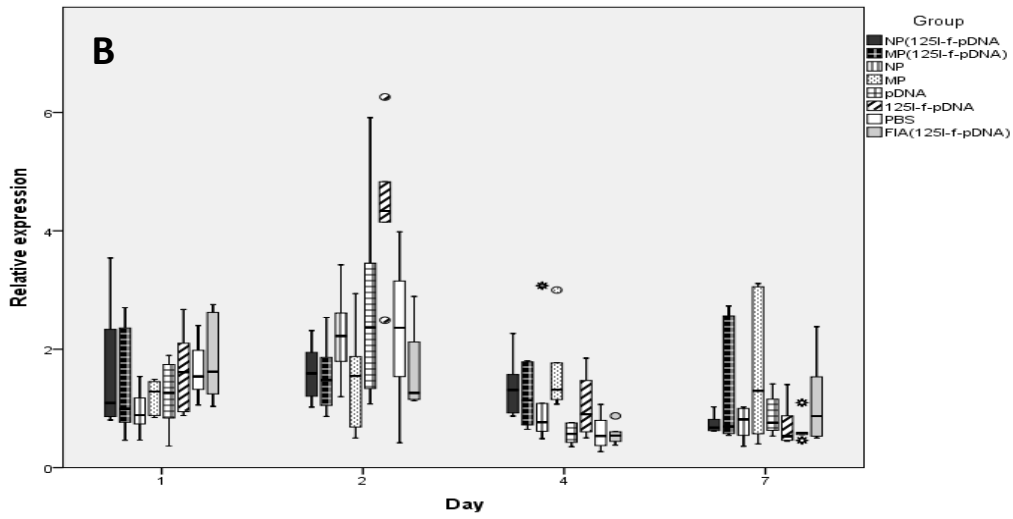
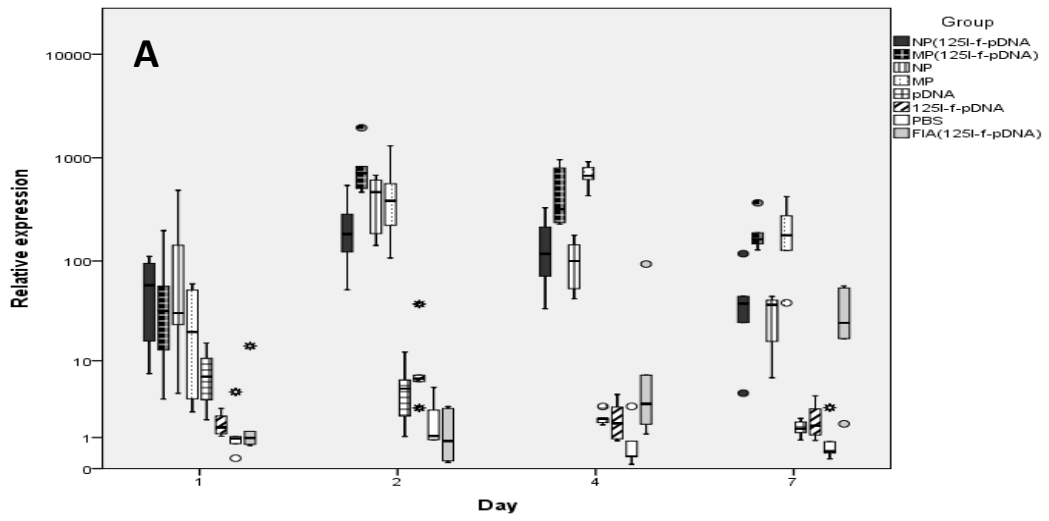


Figure 4 – Relative expression of proinflammatory cytokines; A) IL-1 $\beta$  in muscle from the injection site and B) TNF- $\alpha$  in head kidney. The box-plot shows the median value (line) and maximum and minimum values (whiskers), with the box representing 50% of the samples. Circles show outliers, and asterisks (\*) extreme outliers. Six fish were sampled and analyzed at each time-point.

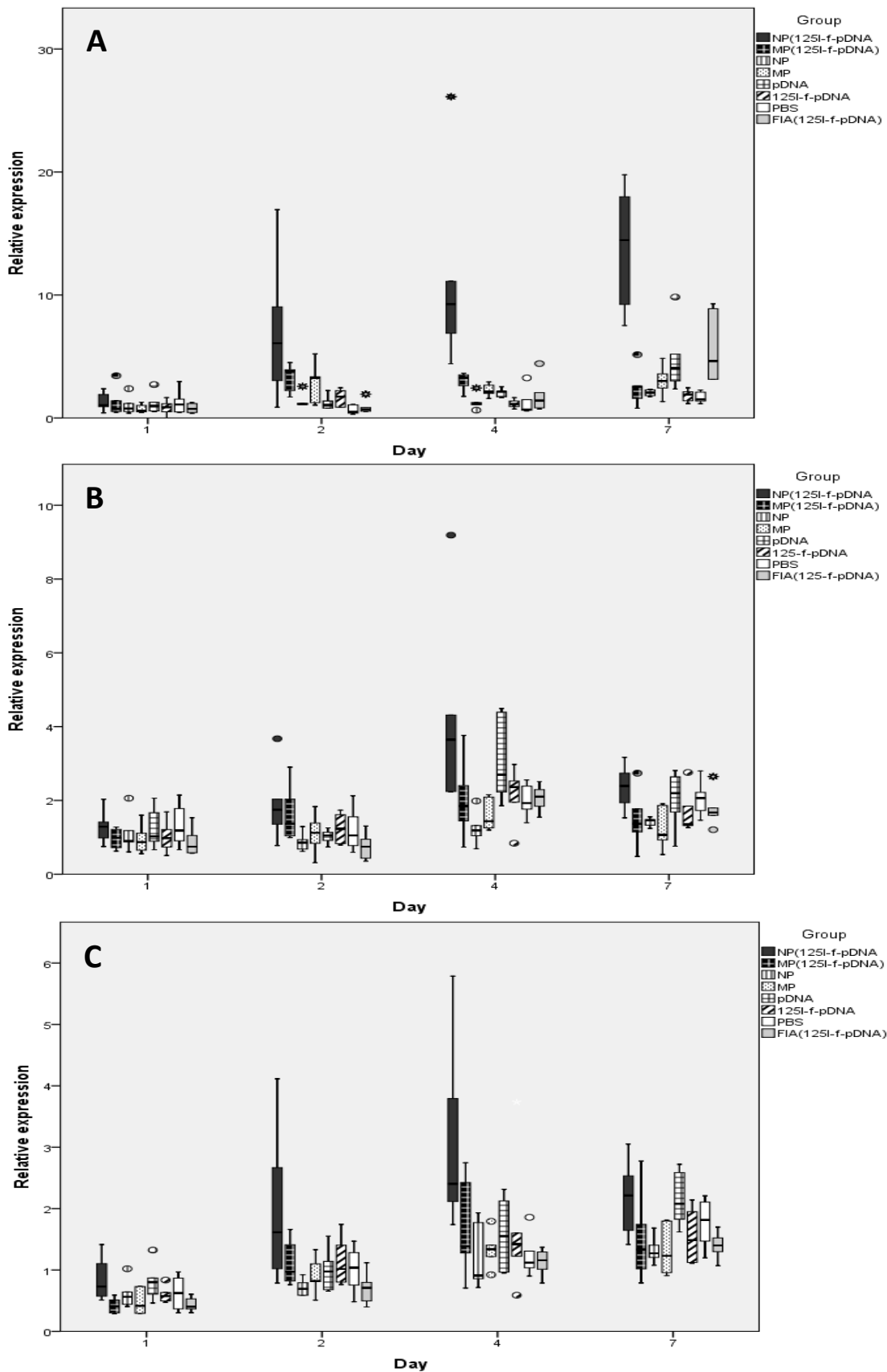
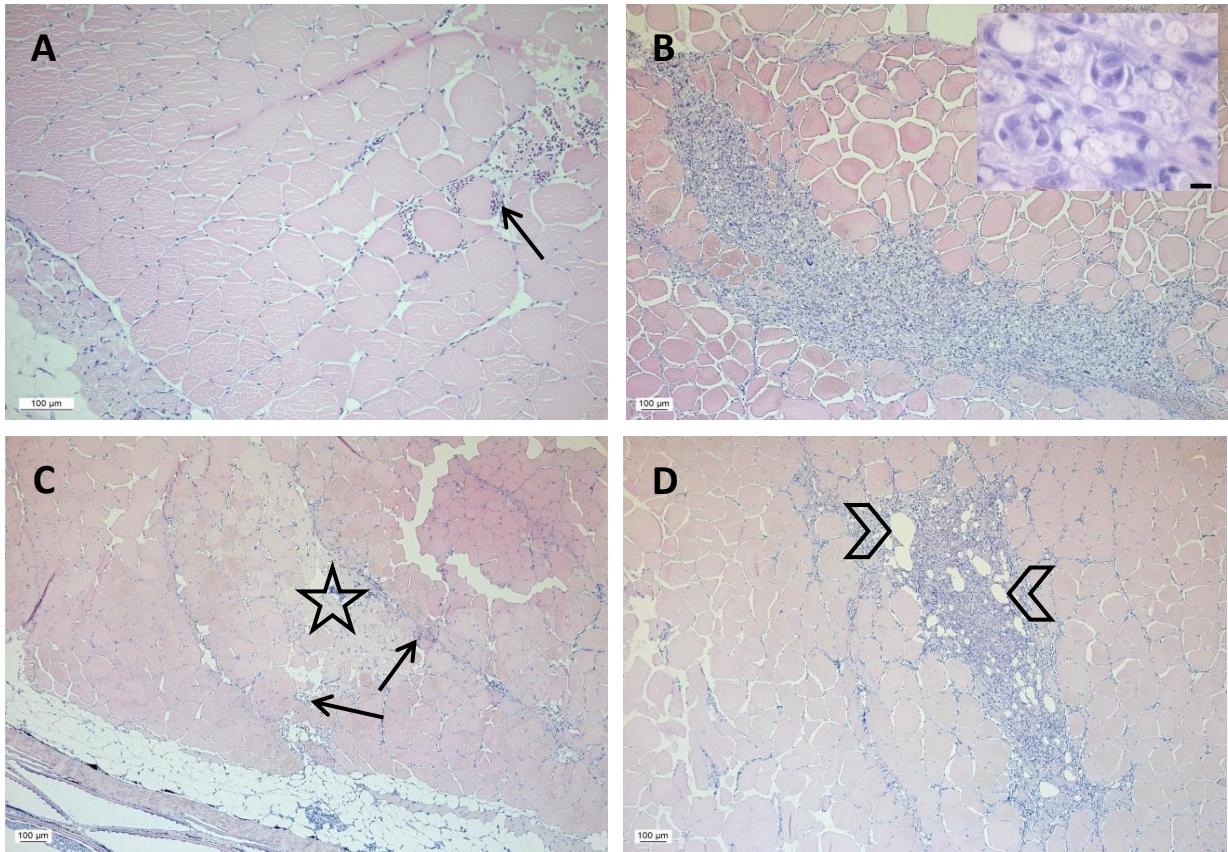


Figure 5 - Expression of the antiviral protein Mx in A) injection site muscle, B) head kidney and C) spleen. The box-plots show median values (line) and maximum and minimum values (whiskers), with the boxes representing 50% of the samples. Circles show outliers, and asterisks (\*) extreme outliers. Six fish were sampled and analyzed at each time-point.



**Figure 6** – All pictures show transversal sections of skeletal muscle from the injection site, stained with hematoxylin and eosin (HE). A) Minor hemorrhages (arrow) and muscle cell degeneration in negative control (PBS) group observed at day 2. B) Massive cellular infiltrate in the myocyte fibre and surrounding interstitium at day 30 in tissue of fish injected with MP-<sup>(125I)-f</sup>-pDNA). Magnification of cellular infiltrate is shown with a 10.0 μm scale-bar. C) Focal muscle cell degeneration (star) and minor hemorrhages (arrows) can be seen at day 7 in samples from fish injected with pDNA. D) Large oil-droplets (arrowheads) surrounded by degenerative muscle fibers and inflammatory cells at day 30 after injection of FIA-<sup>(125I)-f</sup>-pDNA).

**Table 1 – An overview of the preparation protocol and main particle characteristics for pDNA-loaded PLGA nanoparticles (NP-(<sup>125</sup>I-f-pDNA)) and microparticles (MP-(<sup>125</sup>I-f-pDNA)). (S): preparation by sonication. (H): preparation by homogenization. Preparation of empty particles followed the same protocol, but pDNA was excluded from the W<sub>1</sub> phase.**

	NP-( <sup>125</sup> I-f-pDNA)	MP-( <sup>125</sup> I-f-pDNA)
First water phase (W <sub>1</sub> )	pDNA (3.5 mg) in 600 µl dH <sub>2</sub> O with 0.1% PVA	
Oil phase (O)	300 mg PLGA in 6 ml chloroform (5% w/v)	
First emulsion (W <sub>1</sub> /O)	S: 30 sec, 35% (262.5 W)	S: 35 sec, 30% (225 W)
Second water phase (W <sub>2</sub> )	15 ml dH <sub>2</sub> O with 2% PVA	
Second emulsion (O/W <sub>2</sub> )	S: 1 min, 30%	H: 45 sec, 9500 rpm min <sup>-1</sup>
Washing	5000 x g, 15000 x g and 25000 x g	500 x g
Particle yield (%)	78	89
Encapsulation efficiency (%)	27	24
Loading (µg pDNA/mg PLGA)	3.24	2.85
Mean size	320 nm	3-4 µm
PLGA injected (mg)	3.5	4

**Table 2 - Experimental groups and group nomenclature.**

Treatment groups	Nomenclature
( <sup>125</sup> I-f-pDNA) encapsulated in nanoparticles	NP-( <sup>125</sup> I-f-pDNA)
( <sup>125</sup> I-f-pDNA) encapsulated in microparticles	MP-( <sup>125</sup> I-f-pDNA)
Empty nanoparticles	NP
Empty microparticles	MP
Plasmid DNA in PBS	pDNA
( <sup>125</sup> I-f-pDNA) in PBS	<sup>125</sup> I-f-pDNA
PBS	PBS
( <sup>125</sup> I-f-pDNA) in Freund's incomplete adjuvant	FIA-( <sup>125</sup> I-f-pDNA)

**Table 3 - Primers for quantitative polymerase chain reaction (QPCR). (\*): primers obtained from Natasha Hynes (TNF- $\alpha$ ) and Jaya Kumari (Eomes).**

Primer		Oligonucleotides, 5' to 3'	GenBank accession number	Concentration (nM)	Amplification efficiency (%)	Amplicon size (bp)
EF1A <sup>1</sup>	Fw	CACCACCGCCATCTGATCTACAA	AF321836	150	93	78
	Rv	TCAGCAGCCTCCTTCTCGAACTTC		150		
Luc <sup>2</sup>	Fw	TGGGCTCACTGAGACTACATCA	M15077.1	900	100	64
	Rv	CGCGCCCGGTTTATCATC		900		
TNF $\alpha$ <sup>*</sup>	Fw	TGTCCATCAAGCCACTACACTC	BT049358	250	84	129
	Rv	GCACTCACACACCTGTCATT		250		
IFN $\alpha$ <sup>1</sup>	Fw	TGGGAGGAGATATCACAAAGC	NM_001123570	250	89	163
	Rv	TCCCAGGTGACAGATTTTCAT		250		
IL-1 $\beta$ <sup>1</sup>	Fw	GCTGGAGAGTGCTGTGGAAGA	AY617117	200	104	73
	Rv	TGCTTCCCTCCTGCTCGTAG		200		
CD8 $\alpha$ <sup>3</sup>	Fw	CGTCTACAGCTGTGCATCAATCAA	AY693391	200	83	266
	Rv	GGCTGTGGTCATTGGTGTAGTC		200		
Eomes <sup>*</sup>	Fw	ACCTCTCGTCGTCAGATAGTG	NM_001204100	200	82	204
	Rv	GGACCGGTGAGTCTTTTCTTC		200		
Mx <sup>4</sup>	Fw	TGCAACCACAGAGGCTTTGAA	NM_001139918	200	92	79
	Rv	GGCTTGGTCAGGATGCCTAAT		200		

**Table 4 - Histopathological observations in tissue-sections of muscle from the injection site. Muscle degeneration and inflammation are classified as either moderate (+) or strong (++), depending on the extent of the pathology.**

Sampling	Group	Total number of fish	Hemorrhage	Muscle degeneration		Inflammation	
				+	++	+	++
D2	NP-( <sup>125</sup> I-f-pDNA)	3	2	2	0	0	0
	MP-( <sup>125</sup> I-f-pDNA)	3	2	3	0	2	0
	NP	2	1	1	1	0	0
	MP	3	2	0	2	0	0
	pDNA	3	1	1	2	0	0
	<sup>125</sup> I-f-pDNA	3	2	0	0	0	0
	PBS	2	1	2	0	0	0
	FIA-( <sup>125</sup> I-f-pDNA)	1	-	1	-	-	-
D7	NP-( <sup>125</sup> I-f-pDNA)	3	2	2	0	2	0
	MP-( <sup>125</sup> I-f-pDNA)	3	0	3	0	2	0
	NP	2	0	1	1	2	0
	MP	2	1	2	0	2	0
	pDNA	3	1	2	0	1	0
	<sup>125</sup> I-f-pDNA	3	2	1	0	0	0
	PBS	2	0	0	0	0	0
	FIA-( <sup>125</sup> I-f-pDNA)	1	-	-	-	-	-
D30	NP-( <sup>125</sup> I-f-pDNA)	2	0	0	0	2	0
	MP-( <sup>125</sup> I-f-pDNA)	2	0	1	1	0	2
	pDNA	2	0	0	0	2	0
	<sup>125</sup> I-f-pDNA	2	0	0	0	0	0
	PBS	1	0	0	0	0	0
	FIA-( <sup>125</sup> I-f-pDNA)	1	-	-	-	-	1